Dissertation

# STUDY ON EVALUATION METHOD FOR DETERIORATED BRIDGE SLABS BY SELF-PROPELLED IMPACT VIBRATION EQUIPMENT

Graduate School of
Natural Science & Technology
Kanazawa University

Division of Environmental Design

Student ID No.: 1624052003
Name: Nguyen Thu Nga
Chief advisor: Prof. Hiroshi Masuya
Date of Submission: January, 2019

# Abstract

It is well known that almost highway bridges in Japan were built in period 1965-1980 when the Japanese economy grew up rapidly. Currently, there are a significant number of bridges nearly 50 years of age, and their aging has become a massive challenge for maintenance. Fatigue damages of reinforced concrete slabs have been seen not only in Japan but also in developing countries, such as Vietnam, which might be serious problems in future. As of 2008, the mandatory maintenance of bridge deck slabs has taken place every 5 years. After confirming and evaluating the situation through a visual inspection, repair plans and detailed investigations have been carried out. However, material deterioration such as salt damage, frost damage, an alkali silica reaction, and other types of damage have conspicuously appeared, and hence, it is difficult to evaluate the degree of deterioration when focusing solely on cracks. It is necessary to provide reasonable judgment and economic repair methods for highway bridges, which make up a valuable infrastructure in rural areas.

Therefore, in this study, an experiment was conducted on the impact force using self-propelled impact vibration equipment (SIVE), which was developed for highway bridge deck slabs and pavement. The measured values and analysis results using the finite element method (FEM) were then compared, leading to an establishment of a method for evaluating the degree of deterioration.

Also, we propose a method of inserting rods of carbon fibers impregnated with resin in grooves on the lower surface of the concrete slab and confirming the reinforcing effect by the wheel load running experiment.

# Acknowledgement

The author wishes to thank to people, who directly or indirectly contributed to research in this dissertation. Firstly, I want to express my appreciation to my academic supervisor Prof. Hiroshi Masuya, who spent countless hours of his working time with me to do research and sole many academic problems with his ample knowledge. Not only in research but also in daily life, our family was full-filled with the warmest caring of Prof. Masuya and his dearest wife. Secondly, my thesis would be unable to complete without a lot of experiments by cooperation company and distinguished researchers, Dr. Hiroshi Yokoyama. I would like to thank my colleagues in my laboratory, Mr. Takafumi Yamaguchi and Mr. Masashi Kadodera who help me to do experiments and all the laboratory staffs. I want to thank Vietnamese Government for financial support in spite of many difficulties. During the period of 3 years living and studying in Japan, many Japanese people and friends have indicated that my choice to live in Kanazawa city and study in Kanazawa University, could not be better. I appreciate their support and shares all the unforgettable memory. I am thankful to all of family, doctors and friends who are always beside me when I delivered my baby, Last, but not least, I want to thank my family for their unconditional love and support, especially, my beloved daughter. I am the luckiest person to be here with all my grateful for such an opportunity.

# Contents

# List of figures

# List of Tables

# Chapter 1 Introduction

## 1.1 Current status of bridges

After the end of The World War II, in period 1965-1980 Japanese economy grew up rapidly, not only home appliances, but also social infrastructure such as water supply, electricity, roads speedily penetrated society and people. Japan's economic development has been influenced by the achievement of these period.

Regarding this time, almost all highway bridges were built, currently, the are a significant number of bridges nearly 50 years of age and more [1]. These bridges function as a part of a transportation network that is very important such as the Shinkansen and expressway, long-distance flows of people and things, people like the city roads and farm roads, etc. Also, even though there are large and small, each is still being used as a substitute, as an indispensable thing. However, it is about 50 years since the start of service, and after had been used for a long time so far, many bridges where degradation phenomenon was found.

For example, in steel bridges, breakage and cracks of members, corrosion caused by peeling of paint, etc. are observed, and in concrete bridges, corrosion and rupture of steel materials such as cracks and reinforcing bars in concrete parts are seen [2]. In addition, in the Hokuriku region where bridges as targets for research in this thesis, snow melt has been sprayed on the road in winter, and as a material of concrete structures [3], and the occurrence of degradation phenomenon such as cracks due to ASR and salt damage, corrosion of reinforcing bars and leakage in the concrete slabs of many bridges [4]. Therefore, it is important to inspect these bridges, it is said that inspections are carried out as soon as possible, grasping the degradation situation of the deck, and it is necessary to take measures such as repair, reinforcement, or replacement as soon as possible [5].

## 1.2 Study on Damage Evaluation

### 1.2.1 Present status of inspection regulations and systems

Domestic bridges will be checked for the usability and safety of bridges and their performance will be restored according to [1], [6], [7], [8] of the bridge length longevity repair plan formulated by the Ministry of Land, Infrastructure and Transport and local governments [1], [6], [7], [8]. For the detailed procedure of inspection, many local governments throughout the country have standardized bridge periodic inspection procedure [9] defined by the Ministry of Land, Infrastructure and Transport as standard.

This inspection procedure was first established in 1988, and in principle about the frequency of various inspections, it was decided to carry out the visual inspection once in 10 years and the overall inspection once every 2 years. However, in recent years, damages requiring repair are frequently occurred within 10 years after inspection, and since damage has also increased due to deterioration of steel members, a new guideline was enacted in 2004, in accordance with this, regular inspections were conducted once every five years [2]. In addition, the new guidelines also include expressions that suggest the necessity of repair etc. In the explanation of each survey method, and furthermore an inspection conducted in the middle year of the periodic inspection (supplementary inspection) as well as to conduct inspection (specific inspection) on specific events such as salt damage as necessary and devised to more aggressively deal with the deterioration phenomenon of bridges compared with the previous. For reference, the system diagrams of various inspections in the periodic procedure, and the outline of various inspections, regarding the inspection site, it is divided into parts such as the upper structure, the lower structure, the support part, on the road, etc., and each member such as the steel member, the concrete member, and inspects according to the method. In the case of concrete floor slabs, there are many inspection items to be examined in order to maintain the function as a bridge, such as cracking, peeling off, falling off, leakage, discoloration and the conditions of the surface.

The inspection procedure has been revised to meet the current situation, and inspection items are diversified, so it can be said that we are trying to find bridge anomalies at an early stage. On the other hand, there are some problems to be solved in conducting inspections according to the inspection procedure [10].

One of the problems concerning the system of each local government is one of them. Inspections should normally be performed by engineers engaged in bridge conservation work, but among all the municipalities, 50% of the towns and 70% of the villages have no technicians capable of engaging in it. Some of these municipalities also conduct inspections using the original bridge periodic inspection procedure, but about 80% of the municipalities perform only inspections by visual observation, which is a serious. There is a danger of overlooking damage.

Therefore, despite the existence of bridges to be examined, some local governments are not able to conduct satisfactory inspections due to lack of engineers at present.

### 1.2.2 Previous research on soundness assessment

As mentioned, it is considered that development of an inspection method directly related to the determination of performance of bridges is necessary for evaluating bridges without sufficient technology. Several studies related to soundness assessment have been conducted so far.

In the concrete floor slab, research to investigate its fatigue behavior has been carried out in order to obtain knowledge such as fatigue process up to the limit of its use. In the study by Matsui and Maeda announced in 1986 [11], the active load deflection of the RC floor specimen subjected only to the repetitive wheel load increased with increasing number of loads, and the orthogonal anisotropy neglecting the tensile side concrete. When reaching the theoretical value of the plate and the crack density reaches a certain value, it becomes clear that the deck becomes the use limit state, and the decrease in rigidity and the crack density can be an index for estimating the use limit condition of the deck. According to Matsui's research published in 1987 [12], when the RC floor plate test specimen is subjected to repeated wheel loads with water on its upper surface, due to the action of water invading the interior of the slab

from the cracks that appeared during the test, It was revealed that the use limit condition was reached with less loading number and it was suggested that the effect of water invading the inside against the fatigue of the deck also influences. About fatigue of concrete floor slabs accompanied by chemical deterioration such as salt damage and ASR, in the study by Miyamura (2008), Maeshima (2016), when deterioration progress only due to the load burden, it is clear that, the tendency to reach the end at a smaller number of loading times

Based on these studies, researches on the method of determining the degree of degradation have been conducted.

Research has been conducted on an evaluation method utilizing a change in natural frequency of a floor slab due to progress of fatigue, utilizing the fact that deterioration advances to cause a decline in the stiffness of the deck. In the previous study by Miyamura (2008) [13], when RC floor plate specimens undergoing fatigue development were subjected to impact vibration by weight falling and forced vibration by the vibrator. In the case, research was conducted to investigate the change of the natural frequency, and the frequency tends to decrease in higher order vibration mode. According to Makishima announced in 2015, the fatigue test was carried out on the RC slab brought from the actual bridge, and the decrease in the resonance frequency at that time was confirmed at the site where relatively large deterioration such as many cracks. And it was suggested that the decrease of the resonance frequency was remarkable in the part where the damage on the deck was relatively severe.

Research on degradation degree evaluation using active load deflection has also been conducted. In the previous study by Matsui et al. In 1986 [12], the proposal of the degree of deflection has been made, and the idea of ranking the damage level by this is advocated. Based on this idea, research has been conducted to measure live load deflections on actual bridges and investigate whether there is a correlation between deterioration degree, phenomenon of the deck slab and indicating it. As a loading method, static loading due to wheel load and the like can be considered as one plan. However, in order to apply the weight of the apparatus which becomes a wheel load

directly as a load, and in order to give a displacement to the actual bridge, in a general vehicle, it is necessary to install a device having a weight and a size, it takes time and effort to accurately set the vehicle at a predetermined position. Therefore, in recent years, research using shock load caused by dropping a heavy weight has been frequently conducted as a simple method that requires a relatively light equipment installation. Many research using FWD (Falling Weight Deflectometer) as a loading machine have been reported. FWD has been mainly used as a device for structural evaluation of pavement which confirms whether pavement and roadbed are densely laid without a gap [16], [17]. According to Sekiguchi (2003), even one integrated RC slab in an actual bridge, the portion considered to be nearly finished in a remarkable part of the damage with penetrating cracks. The displacement distribution around the loading point is not a parabola but a distribution when punching shear fracture occurred and locally grasps the damaged portion that can affect the load carrying capacity of the deck by FWD was suggested that it could be done. According to Yamaguchi (2015) [19], the degree of deterioration due to active load deflection of the RC slab of the actual bridge generated by FWD and the degree of deflection in the central deflection relative to the deflection magnitude at positions other than the center at the time of live loading. The relation of the ratio was examined, and the degree of damage at each position on the deck was judged. In addition, research to investigate the displacement of the floor slab by the falling of the weight, a study in which impact loading is carried out using a compact FWD called IIS, and the displacement of the deck at that time is examined by a speedometer [20], [21]

However, the loading machine used in these studies has several problems. In the case of FWD, most of them are on-board type, and measurement of loading point displacement is carried out by displacement meters installed on the lower surface of the floor plate, so in many measurement methods reported so far. It takes time and effort to install the machine and the displacement gauge, so it is considered that it is difficult to measure more quickly. With intelligent infrastructure system, installation of measuring instruments related to displacement measurement such as speedometer

is relatively simple, but because the loaded load is small, it is difficult to excite a bridge with high rigidity.

### 1.3 Study on new structure of bridge

#### 1.3.1 Current status of repair and reinforcement of the deck

Judgment of necessity of repair, reinforcement or replacement in each bridge is carried out at the time of periodic inspection based on the inspection procedure. Moreover, it is decided that correspondence is made according to each judgment classification. Regarding the inspection status of recent bridges, among the bridges with the highest priority for inspection managed by all domestic road, up to 2016, 54% inspections are done at bridges, and judgments are made. However, those bridges that are judged to be required correspondence such as repair, reinforcement, and replacement, but only a few have actually responded to them.

For those judged by the end of 2015, only a small number of those bridges are repaired or reinforced, and other bridges of the same condition are not under planned. Other condition of bridge such as under limit of usability, although some response has been completed or will be done, about 50% of responses such as repair and replacement are still decided, others are removed. There are some bridges that have not yet been dealt with sufficiently, such as abolition or undecided correspondence [22], owing to the lack of engineers and financial shortage.

Almost all the highway bridges were built after the period of high economic growth, and these years aging has progressed years after years, on the other hand, the budget for responding to some kind of bridge has been decreasing year by year. In recent years, the declining birthrate and aging of society is proceeding, and reduction of labor force for treatment is also a reason. Therefore, in this situation it is necessary to it may fall into a situation of paralyzing the nationwide transportation network.

#### 1.3.2 New structure

As a condition of the new structure to be applied, the repair reinforcement cycle is shorter than the conventional structure, and it is easy to construct with less expense. Specifically, those in which factors causing cracks has been removed or precast type

structures will apply to them. There are some structures that devised to suppress cracks. As an example, in order to suppress corrosion of reinforcing bars, there are structures using reinforcing bar coated with epoxy resin and painted on concrete surface to prevent intrusion of chloride ions [23]. The other cases of pretensioner girder construction using CFRP (Carbon Fiber Reinforced Polymer) as reinforcement method which is made of nonferrous material. It is said that CFRP is lighter than reinforcing bar and fewer possibility of corrosion occurrence. Although there is a girder bridge using CFRP for 30 years, observed no occurrence of harmful deterioration at the bridge until now.

## 1.4 Theme of this thesis

### 1.4.1 Damage evaluation of actual bridge deck slab using impact load caused by FWD

Owing to all these advantages and disadvantages we will introduce Self-propelled Impact Vibration Equipment (SIVE) as a loading machine and conduct experiments. SIVE is a loading machine that gives impact force by dropping a weight loaded with FWD, but the difference from the conventional in-vehicle FWD is that loading is impossible in the past because the loading machine is moved by a small crane. It also possible to load at the end of the road surface and make fine adjustments to fit the loading board to the loading point, as it also benefited from small turning, making the choice of loading points wider. In addition, in order to save labor in installing the displacement measuring device, we decided to adopt a system that uses a placement type accelerometer for the displacement measurement and calculates the second order integral value of the measured acceleration as the measurement displacement. Furthermore, the accelerometer was arranged at regular intervals in the direction of the girder, and displacement was measured in the form of displacement distribution. Actual tests were mainly carried out on the RC slab of the actual bridge. SIVE (Self -propelled impact vibration equipment) was developed to evaluate the deterioration of slab simply and rationally. This equipment can change the mass of falling weight, a height and a rubber condition used as cushion system. When SIVE is used at the site, generally, proper impact force, momentum and duration of impact force are

required depending on the scale of objective structure. In this study, impact tests for series of rubber buffer were performed, characteristics of impact force were shown and summarized.

Also, in order to ascertain what degree of deterioration of the experimental value is, we compared it with calculated value and analysis value.

### 1.4.2 Experimental Study on reinforcement effect by carbon fiber for fatigue-damaged concrete deck.

The number of aging bridges increases certainly in Japan, maintenance and management of them become an unavoidable social issue. Therefore, the planning of effective countermeasures for damaged bridge is one of urgent important issues. In the present situation, the bridge inspection legislated in 2014 has been proceeding in Japan [24,25]. The grasp of damage degree and implementation of repair countermeasures corresponding the results of bridge damage have been executed mainly on the national highway.

However, the most of domestic bridges under local municipal management actually are not efficiently taken care due to lack of engineers and financial shortage. It is considered necessary to give a reasonable judgment method to select two ways, which specifically is the way ensuring the required performance by repair and reinforcement and the way prolonging the life until the next countermeasure [26,27].

Therefore, in this research, in order to provide the reinforcement method to improve load bearing performance and the method that can be expected to prolong life even if improvement of load bearing performance cannot be anticipated, experimental research had been done.

References

[1] Hokuriku Regional Development Bureau, Ministry of Land, Infrastructure and Transport: Bridge length longevity repair plan, pp.1 - pp.13, 2014.1

[2] Takashi Tamakoshi, Akira Ohashi, Shoichi Nakatani: Reference materials on periodic checks on roads - Photograph collection of bridge damage cases photo book -, National Land Technology Policy Research Institute Document No. 196, 2004.12

[3] Katsunobu Takeuchi, Maki Kawamura, Kazuyuki Torii Torayama: Prediction of Tissue and Residual Expansion of Concrete Degraded by Alkali Silica Reaction, Materials of Japan Society of Materials, Vol. 43, No. 491, pp. 963 - pp. 969 , 1994.8

[4] Torii Kazuyuki, Sasaya Teruhiko, Kubo Yoshiji, Sugitani Shinji: Investigation of ASR Damage Level of Bridges Affected by Freezing Preventives, Concrete High School Years' Collection, Vol.24, No. 1, 2002

[5] Ministry of Land, Infrastructure and Transport: efforts to counter aging, browsing in November 2017

http://www.mlit.go.jp/road/sisaku/yobohozen/torikumi.pdf

[6] Kanazawa City Civil Engineering Bureau Road Management Division: Kanazawa City Bridge Long-Term Repair Plan, 2012

[7] Ishikawa Prefecture civil engineering department road maintenance division; pavement maintenance repair group: Ishikawa prefecture bridge long life improvement repair plan [change], 2014.3

[8] Toyama prefecture civil engineering department: Toyama prefecture bridge length longevity repair plan, 2017.3

[9] National Highway and Disaster Management Division, Ministry of Land, Infrastructure and Transport Road Bureau: Bridge regular inspection procedure, 2014.6

[10] Hokuriku Regional Development Bureau: Recent efforts of the Hokuriku Regional Development Bureau, Forum on repair and reinforcement of concrete structures, 2016.8.17

[11] Shozo Matsui, Yukio Maeda: Proposal of Degradation Determination Method for Road Bridge RC Deck, Proceedings of JSCE 374 / I-6 pp. 419 - pp. 425 1986. 10

[12] MATSUI Shigeyuki: On the fatigue strength and the influence of water on road bridge RC floor slab subjected to moving load, Report on Concrete Engineering Annual Papers 9-2 pp. 627 - pp. 632, 1987

[13] Miyamura Masaki, Koda Yasuhiro, Naito Hideki, Iwaki Ichiro, Suzuki Motoyuki: Study on Evaluation Method of Fatigue Damage Level of RC Deck Floor Focusing on Vibration Characteristics, papers of Structural Engineering Vol.57A pp.1251-1262, 2011

[14] Masajima Taku, Maeda Yasuhiro, Ichiro Ichiro, Naito Hideki, Kishi Ryuu, Suzuki Yoron, Ohta Koji, Suzuki Motoyuki: Influence of Alkali Silica Reaction on Fatigue Resistance of Road Bridge RC Slabs, Proceedings of the Japan Society of Civil Engineers E2 (Material · Concrete Structure), Vol.72, No. 2, pp. 126 - pp. 145, 2016

[15] Taku Majima, Hideki Naito, Yasuhiro Iwashiro, Ichiro Suzuki: Fatigue Damage Evaluation of Actual Road Bridge RC Slab with Focus on Decreasing Resonance Frequency, The Journal of Structural Engineering of Japan Society of Structural Engineering Vol. 61 A, pp. 778 - pp. 787, 2015.3

[16] Abe Nagato, Maruyama Haruhiko, Himen Kenji, Hayashi Masanori: Structural evaluation of pavement based on deflection evaluation index, papers of JSCE No.460 V-18 pp.41-pp.48, 1993.2

[17] General Association of Japan Road Construction Industry Association: FWD (pavement structure evaluation equipment) viewed in January 2018

http://www.dohkenkyo.net/pavement/kikai/fwd.html

[18] Mikio Sekiguchi, Katsuro Kunifu: Investigation of the soundness evaluation method of the deck by FWD, The Third Symposium on Road Bridge Decking Papers pp.145 - pp.150, 2003.

[19] Yamaguchi Kyohei, Hayasaka Yohei, Soda Nobuo, Onishi Hiroshi: Study on soundness evaluation method of existing RC deck using FWD, papers of Structural Engineering Vol.61 A pp.1062-pp.1072, 2015.3

[20] Yokoyama Hiroshi, Ishige Mari, Tambo Takashi: Experimental Study on Degradation Deterioration of RC Deck by Impact Load, JSSST Structural Engineering paper vol.62A pp.1194-pp.1201, 2016.3

[21] Mikio Sekiguchi, Kyohei Sasaki: Evaluation of the soundness of various floor plates by IIS, 2007 Annual Report on the Civil Engineering Technology Center Annual Report, 2007

[22] Ministry of Land, Infrastructure and Transport Road Bureau: Annual Report on Road Maintenance, 2017.8

[23] Kiyonaki Kiyoshi: measures against salt damage in concrete bridges 30 years history and verification in Japan, materials and environment 59 pp.195 - pp. 204, 2010

[24] Japan road association: Design specifications for steel highway bridges/Production specifications for steel high-way bridge, Gihoudo Co. Ltd., 1956.

[25] Japan road association: Specifications for highway bridges part2 steel bridges ver. 2002, Maruzen Co. Ltd., 2002.

[26] Masuya, H., Yokoyama, H., Sekiguchi, M., and Xu,C.: Study on impact behavior of fatigue deteriorated reinforced concrete slab by finite element method" Proceedings of 11th International Conference on Shock & Impact Loads on Structures, 267-272

[27] Nguyen T., N., Masuya, H., Xu, C., Kaii, H., Yamaguchi, T. and Yokoyama, H.: Self-propelled impact vibration equipment for the utilization of inspection of bridge deck, Proceedings of 9th symposium on decks of highway bridge, pp.89-92, Nov. 2016

# Chapter 2: Development of Self- propelled Impact Vibration Equipment.

## 2.1 Self- propelled Impact Vibration Equipment

### 2.1.1 Overview of SIVE

Falling weight deflectometer (FWD) test has been used widely for evaluation structural with many types. The popular types of FWD are: FWD car, light FWD… Even though the FWD, which is the best nondestructive equipment, still could not fully represent the conditions of moving trucks load. In this study, SIVE (Self - propelled impact vibration equipment) was developed to evaluate the deterioration of slab simply and rationally. This equipment can change the mass of falling weight, a height and a rubber condition used as cushion system. When SIVE is used at the site, generally, proper impact force, momentum and duration of impact force are required depending on the scale of objective structure. In this study, impact tests for series of rubber buffer were performed, characteristics of impact force were shown and summarized. Generally, a certain equipment which has a feature of mobility and enough power to carry out a field test on an entire bridge or a part of bridge, such as a slab deck, is required. Therefore, an equipment (SIVE) was developed to fulfill such requirements.

The overview of SIVE is shown in Figure 2.1. It is easier to set SIVE at any point by a simple operation compared with FWD car systems

This equipment consists of two large parts which are a forklift truck and an impact occurrence equipment. Electric truck works by the battery DC 24 volt and supplies necessary power to the impact occurrence equipment, the measuring equipment and personal computer. The occurrence equipment consists of the hoist lifting a weight, steel weight, rubber buffer, load cell and loading plate. The equipment can change the mass of a falling weight, a falling height and a rubber cushion used in cushion system. The maximum falling height is 0.3 m and the maximum mass of weight is 220 kg. The capacities of energy and momentum are 0.65 kJ, 0.44 kNs respectively.

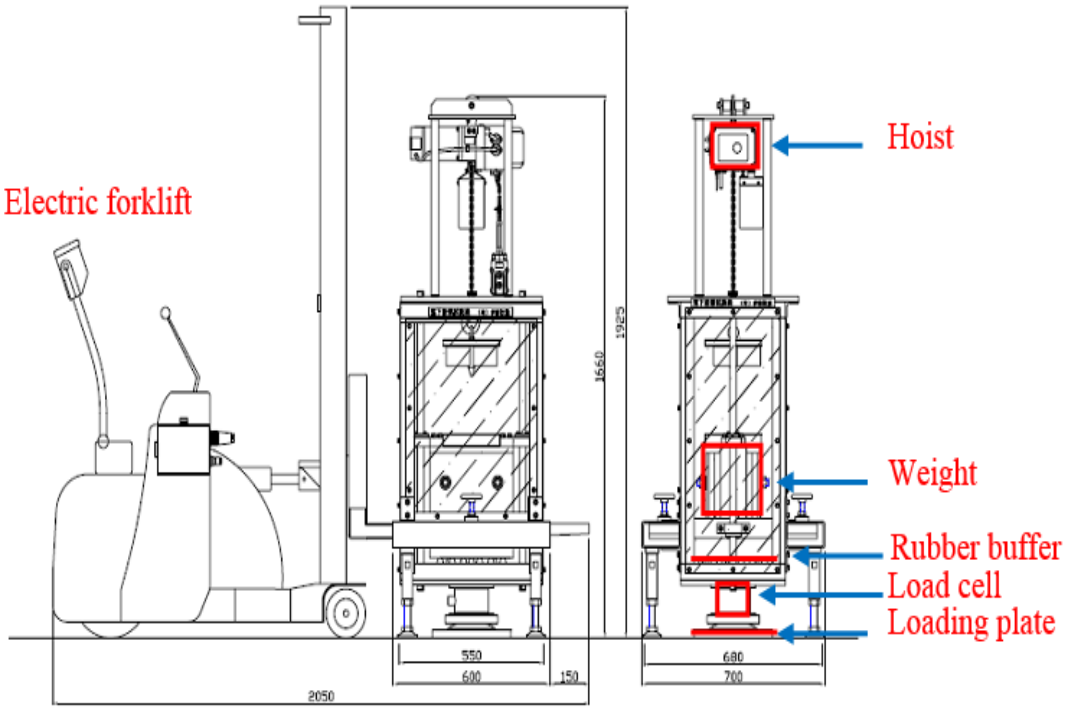


**Figure 2.1: Overview of SIVE (Self -propelled Impact Vibration Equipment)**

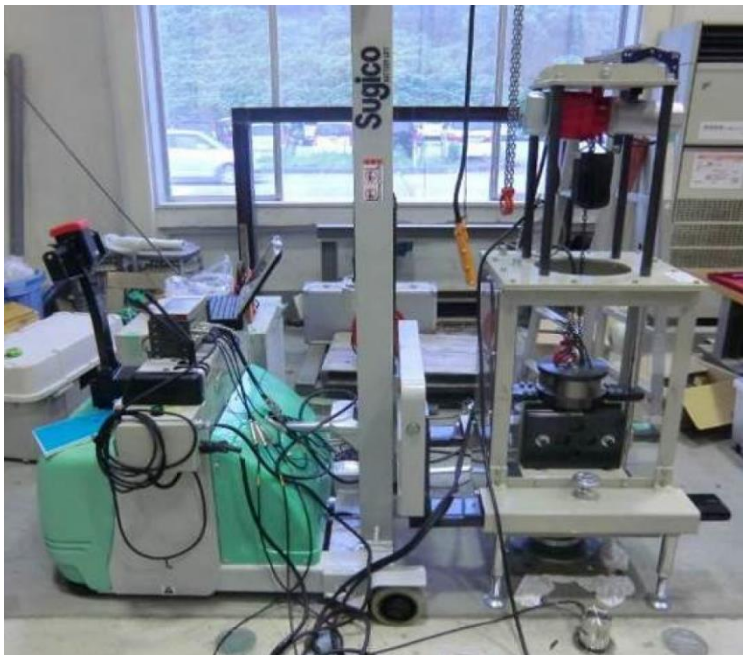


**Figure 2.2: SIVE**

### 2.1.2 Loading method

The structure of the loading machine is shown in Figure 2.3. For weight placement before loading, lift the weight with a hoist to a prescribed height with an electric magnet and place it at that height with the weight held up until it is dropped. The

weight fall is performed by releasing the magnetic force of the electromagnet and releasing the weight. The falling weight collides with the shock absorber installed directly below. The impact force generated by the collision is transmitted to the road surface where the loading board is in direct contact via the load cell installed on the lower side of the shock absorber and the loading board to generate the displacement of the floor slab.

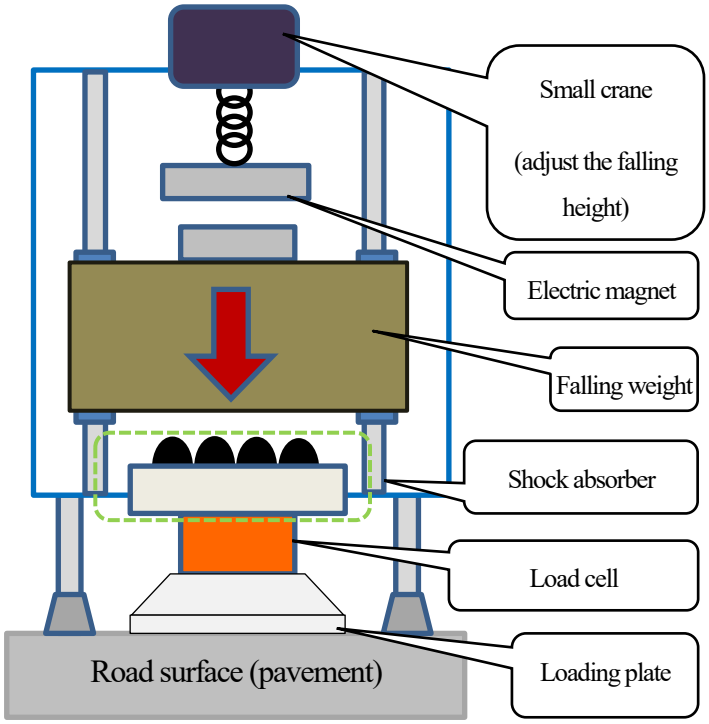


**Figure 2.3: Impact occurrence part**

The impact load at the loading point was measured using the load cell inside the loading machine described above. Figure 2.4 shows the load cell. The capacity is ± 500 kN, and it is installed at a position sandwiched between the shock absorber and the loading board.

**Figure 2.4: Load cell (Tokyo Instrument KCE-500kNA)**

**Figure 2.5: Acceleration meter (Tokyo Instrument ARJ-200A)**

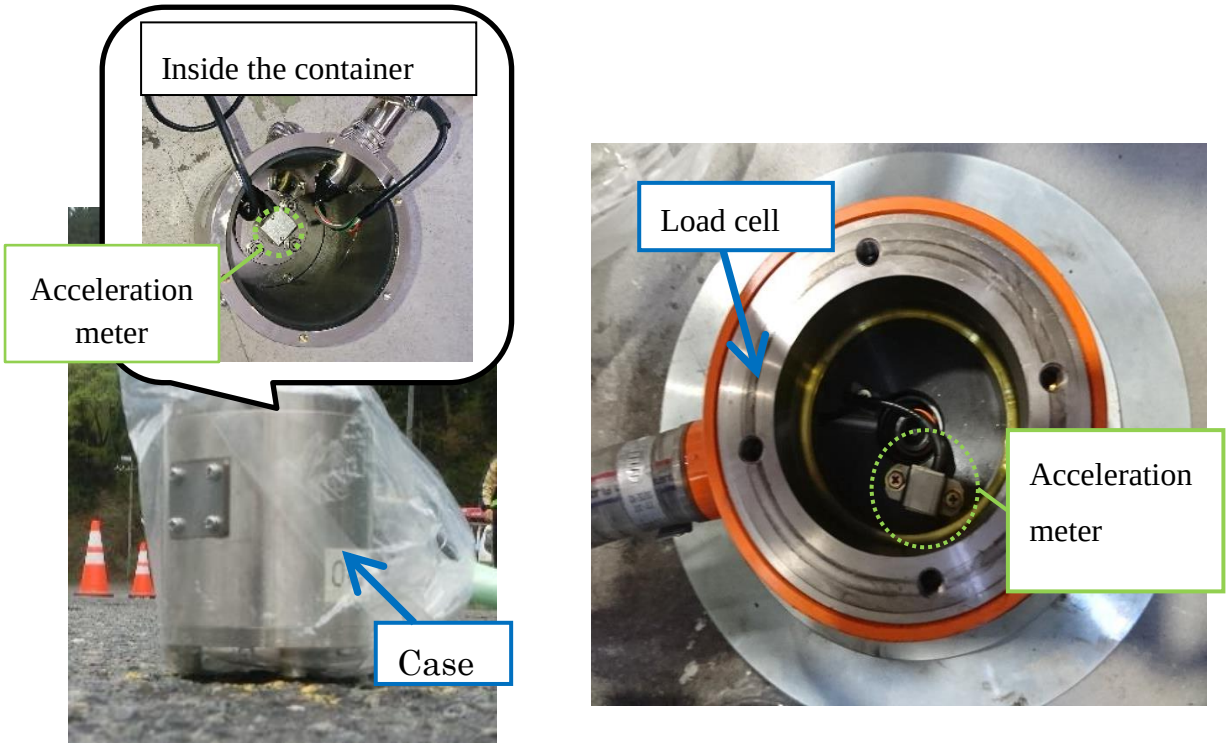


**Figure 2.6: Acceleration meter installation**

### 2.1.3 Displacement measure method

The displacement of the deck was measured using an accelerometer. The accelerometer is shown in Photo 2.5. The displacement is ± 200 m / s $^2$, the displacement of each measurement point is measured by the accelerometer at the installation position, and the value obtained by integrating the measured value on the second order with respect to time is obtained as the measurement displacement. Detailed acceleration integration method is described on the following section. The

measured displacement by the accelerometer shows the absolute displacement of the deck including the displacement of the spar, and the relative displacement of only the deck is obtained by subtracting the value considering the displacement of the digit from the absolute displacement.

Regarding the installation method, the accelerometer other than the loading point by shock loading is included in the case as shown in Figure 2.6 and the case is settled on the road surface at the measurement point. The accelerometer at the loading point position is installed in the empty space of the loading machine load cell as shown in Figure 2.6. In this way, although the measurement position of the floor slab displacement is on the pavement, since it is thought that the girder and the deck will exhibit the same displacement distribution as the pavement at the time of impact loading, the displacement of the girder and the deck slab measurement.


**Figure 2.7 Measurement logger**

The instrument shown in Figure 2.7 was used as a measurement logger. This logger, the load cell and each accelerometer are connected by wires.

As reference measurement method, we attempted not only the displacement measurement of the floor plate from the pavement by the accelerometer but also the displacement measurement from the lower surface of the deck. As a measuring equipment, a displacement gauge and a laser displacement meter were used, and these displacement meters were applied to displacement measurement on the lower surface of a part of the bridge deck.

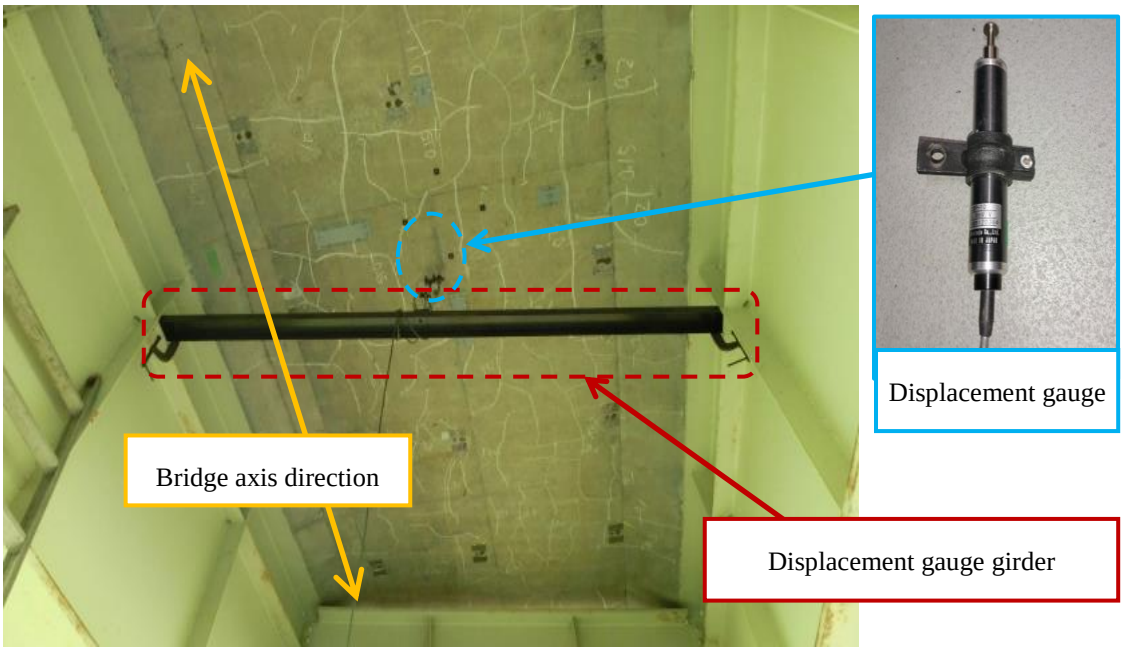


**Figure 2.8: Displacement gauge installation**

A displacement gauge with a range of ± 10 mm was used. The installation method, as shown in Figure 2.8, the bars were placed between bridge and fixed by using vise so as not to move in the vertical direction. As a result, relative displacement of the floor slab was measured. The measurement logger of this, like the other equipment mentioned above, the logger of Figure 2.7 was used.

**Figure 2.9: Laze displacement meter installation**

The laser displacement meter was installed on the riverbank under the floor as shown in Figure 2.9. Regarding the method of measuring the displacement, the laser was emitted and reflected on the deck, the speed was measured from the time it sensed by the laser displacement meter, processing such as integration was performed, and the

value was obtained as measured displacement. Also, a logger different from the one in Figure 2.7 is used for the measurement logger of this displacement gauge, and it is not synchronized with the other measuring instruments mentioned above at the time of measurement.

### 2.1.4 Rubber cushion

The figure 2.10 shows the arrangement of 5 types of rubber cushion for choosing the suitable rubber to control the maximum forces and duration of impact

Type A

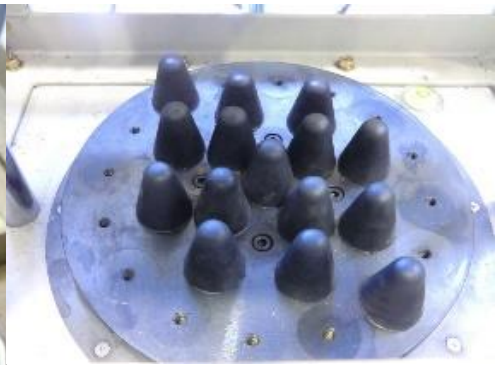

Type B

Type C

Type D

Type E

**Figure 2.10: Rubber buffer**

Type A and B There were 29 and 15 of rubber cones were arranged in Type A and B respectively. This type of rubber cone (rubber buffer KFDF-51, Tokyo sokki kenkyujo co. ltd) is normal rubber, 48 mm of height, 40 mm of diameter. Type D and E are low rebound rubber (Hanenaito, Naigai rubber industry co. ltd.) with the height is 32 mm and the diameter are 26.09 mm. In addition, type C arranged by 6 low rebound triangle rubbers.

### 2.2 Experiment by SIVE

#### 2.2.1 Experiment outline

The series of impact experiment using SIVE were done. Table 1 shows the list of experiments. In this series of experiment, the 220 kg mass of weight is used three times for each case. Experiments were conducted with a plate that has detail of dimensions (Figure 3). The plate was setup in two support, loading plate was set in the center of plate. Displacement of the center point of the plate was measured by a displacement meter (CDP5, Tokyo- sokki kenkyujo co. ltd.).

In the same conditions and five types of rubber, data were collected from equipment built-in load cell. Velocities and displacements were got by using numerical integrations.

**Table 1: List of experiments**

| Cushion Type | Mass of weight | Falling height | Collision energy | Momentum |
|---|---|---|---|---|
| | $M_w$ (kg) | $H_f$ (m) | $E_{ini}$ (kJ) | $M_{ini}$ (kNs) |
| A | 220 | 0.05 to 0.30 | 0.11 to 0.66 | 0.22 to 0.53 |
| B | 220 | 0.05 to 0.30 | 0.11 to 0.66 | 0.22 to 0.53 |
| C | 220 | 0.05 to 0.30 | 0.11 to 0.66 | 0.22 to 0.53 |
| D | 220 | 0.05 to 0.30 | 0.11 to 0.66 | 0.22 to 0.53 |
| E | 220 | 0.05 to 0.30 | 0.11 to 0.66 | 0.22 to 0.53 |

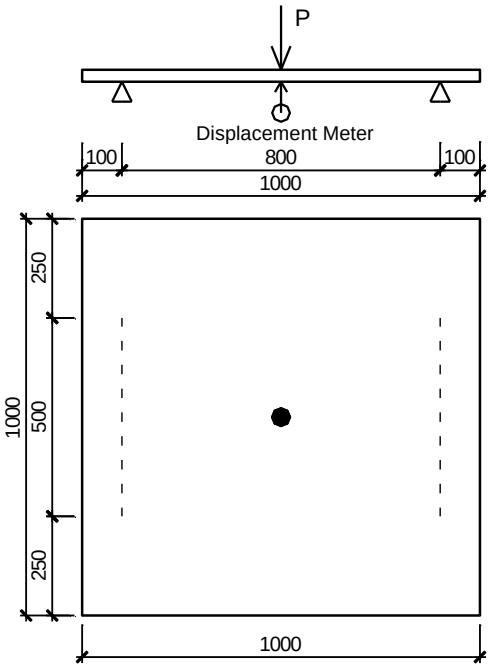


**Figure 2.11 Test specimen**

### 2.2.2 Experiment results

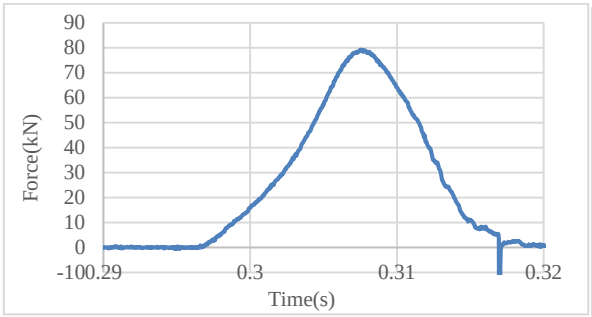


(a) Impact force

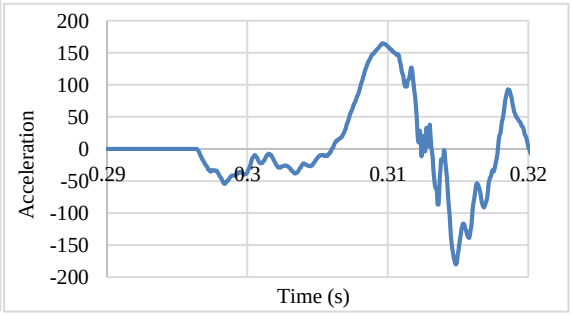


(b) Acceleration

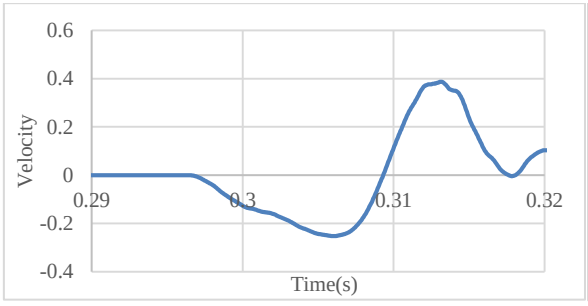


(c) Velocity

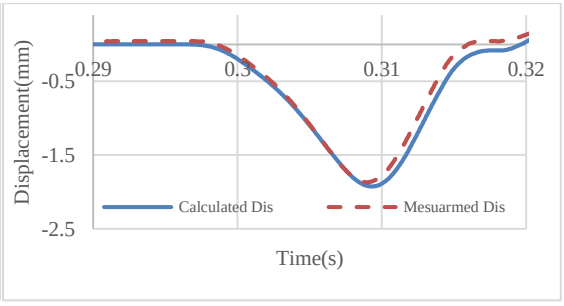


(d) Displacement

**Figure 2.12: Example of impact force, acceleration, velocity and displacements ($M_w$=220 kg, $H_f$=0.3 m, Cushion Type D)**

Figure 2.12 a and b show the time course impact force from 0.3 m height in case of type D rubber and the acceleration data. The first impact is the most important for the dynamic behavior of structure. Thus, the first impact should be focused. In this type of cushion, the impact force reached the peak at about 80 kN in only 0.02 s. With rebound rubber, the rebound of falling weight seems to be reduced. In addition, the velocity was calculated from the acceleration in figure 4c. The displacements measured by the displacement meters and calculated based on acceleration were shown in figure 4d. It became clear that the displacement calculated from acceleration at the center point is in good agreement with the value by displacement meter. The ratio between them was approximately 1.0.

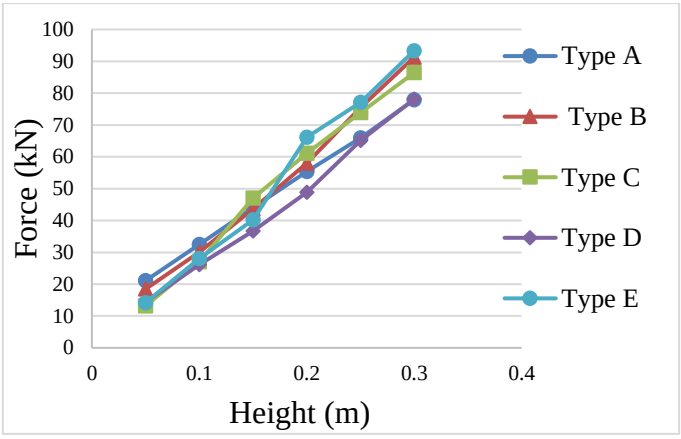


(a) Impact force

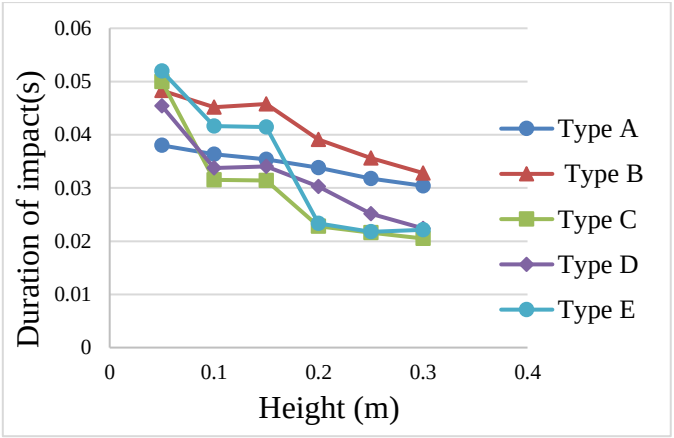


(b) Duration of impact

**Figure 2.13: First impact force and duration of impact**

Figure 2.13 shows the maximum force and duration of impact of different falling heights on all type of cushions. It shows that the maximum force has monotonously increased with the rise of falling heights in all type of cushions. Cushion Type B, C, D and E had experienced some dramatic changes in duration of impact while cushion

Type A had slight one. Different cushions differ in duration of impact and forces. The largest impact force was found in type E cushion. Duration of impact, on the other hand, has decreased along the falling heights.

Figure 2.14 indicates the sample of impulse by the first impact of two typical type of cushion A and D. The maximum force and the duration of force are approximately 90 kN and 0.03 s in both types. It can be seen that rebound is large in Type A (normal rubber) and small in Type D (low rebound rubber).

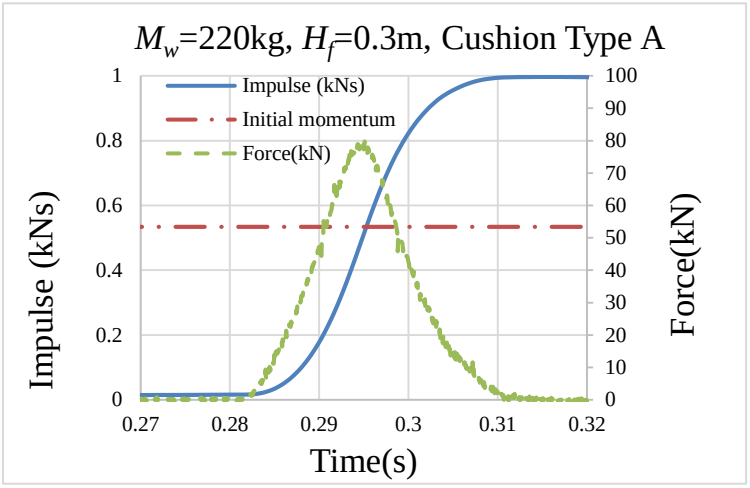


(a) Type A

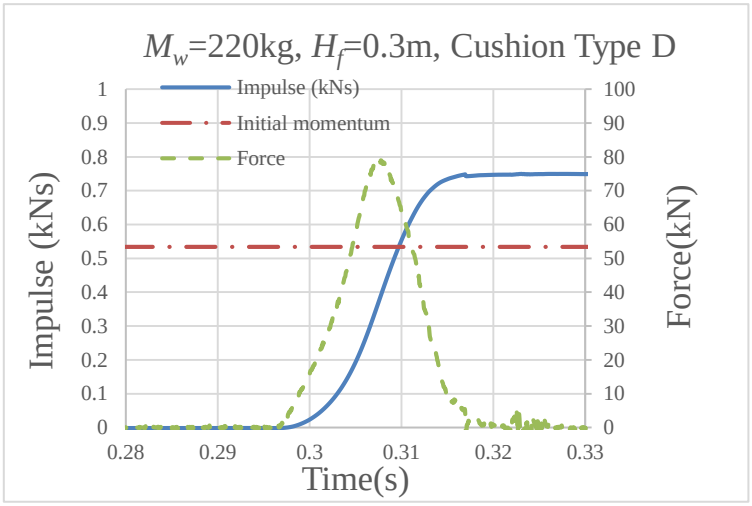


(b) Type D

**Figure 2.14: Sample of impulse and force**

Table 2 provides the overall view of displacement. The difference between the calculated displacements and the true value is small in all case except the one with a low falling height 0.05 m. Displacements experienced the same trend of increase in all case with the rise of falling heights

It generally suggests that it was so important to control the maximum force, duration of force and less rebound of falling weight for better pursuit of experiment at site.

**Table 2: Relationship between calculated displacements and measuarmed displacements**

| Height (m) | | Type A | Type B | Type C | Type D | Type E |
|---|---|---|---|---|---|---|
| 0.05 | $D^{C}_{max}$ (mm) | -0.579 | -0.483 | -0.399 | -0.396 | -0.285 |
| | $D^{m}_{max}$ (mm) | -0.552 | -0.425 | -0.345 | -0.358 | -0.305 |
| | $D^{C}_{max}/ D^{m}_{max}$ | **1.049** | **1.136** | **1.158** | **-1.106** | **0.934** |
| 0.1 | $D^{C}_{max}$ (mm) | -0.815 | -0.812 | -0.926 | -0.648 | -0.068 |
| | $D^{m}_{max}$ (mm) | -0.888 | -0.743 | -0.771 | -0.620 | -0.068 |
| | $D^{C}_{max}/ D^{m}_{max}$ | **0.918** | **1.093** | **1.201** | **1.045** | **1.004** |
| 0.15 | $D^{C}_{max}$ (mm) | -1.092 | -1.115 | -1.252 | -0.868 | -1.033 |
| | $D^{m}_{max}$ (mm) | -1.115 | -1.068 | -1.154 | -0.803 | -1.035 |
| | $D^{C}_{max}/ D^{m}_{max}$ | **0.980** | **1.044** | **1.084** | **1.081** | **0.998** |
| 0.2 | $D^{C}_{max}$ (mm) | -1.311 | -1.487 | -1.616 | -1.160 | -1.705 |
| | $D^{m}_{max}$ (mm) | -1.305 | -1.460 | -1.553 | -1.147 | -1.721 |
| | $D^{C}_{max}/ D^{m}_{max}$ | **1.005** | **1.019** | **1.041** | **1.012** | **0.990** |
| 0.25 | $D^{C}_{max}$ (mm) | -1.620 | -1.870 | -2.001 | -1.576 | -1.985 |
| | $D^{m}_{max}$ (mm) | -1.603 | -1.869 | -1.856 | -1.567 | -1.986 |
| | $D^{C}_{max}/ D^{m}_{max}$ | **1.011** | **1.000** | **1.078** | **1.006** | **1.000** |
| 0.3 | $D^{C}_{max}$ (mm) | -1.947 | -2.241 | -2.358 | -1.927 | -2.569 |
| | $D^{m}_{max}$ (mm) | -1.840 | -2.268 | -2.276 | -1.869 | -2.462 |
| | $D^{C}_{max}/ D^{m}_{max}$ | **1.058** | **0.988** | **1.036** | **1.031** | **1.044** |

### 2.2.3 Experiment conclusion

The maximum forces and durations of impact by SIVE were concretely shown for 5 types rubber cushions. Generation of ideal single impact is possible, when low rebound rubber cushion (Type C, D or E) is used. The maximum force can be controlled bellow 100 kN and duration of impact are approximately 0.2 s to 0.5 s. It is possible to calculate the accurate displacement by the acceleration measured in SIVE.

With the accuracy we will us SIVE for the measurement of displacements at actual site in the future.

## References

[1] Japan road association: Design specifications for steel highway bridges/Production specifications for steel highway bridge, Gihoudo Co. Ltd., 1956.

[2] Japan road association: Specifications for highway bridges part2 steel bridges ver. 2002, Maruzen Co. Ltd., 2002.

[3] Masuya, H., Yokoyama, H., Sekiguchi, M., and Xu,C. “Study on impact behavior of fatigue deteriorated reinforced concrete slab by finite element method” Proceedings of 11th International Conference on Shock & Impact Loads on Structures, pp 267-272,2015.

# Chapter 3: STUDY ON INSPECTING REAL BRIDGE DECK BY SEVERAL FALLING WEIGHT DEFLECTOMETER SYSTEMS

## 3.1 Hinoki bridge

### 3.1.1 Experiment outline

In this study, SIVE (Self -propelled impact vibration equipment) was developed to evaluate the deterioration of slab simply and rationally. This equipment can change the mass of falling weight, a height and a rubber condition used as cushion system. When SIVE is used at the site, generally, proper impact force, momentum and duration of impact force are required depending on the scale of objective structure. Hinoki bridge is constructed in Ishikawa Prefecture in 1973 is a bridge passing through Shiramine, which is a mountainous area of Hakusan City, and is a composite plate girder bridge with one RC on which four RC slabs are placed on the main girder. The cross-sectional view and the plan view of the bridge are shown in Figures 3.1 and 3.2. The bridge length is L = 35,800 mm, and the total width is B = 9200 mm. The width of roadway is 7000 mm.

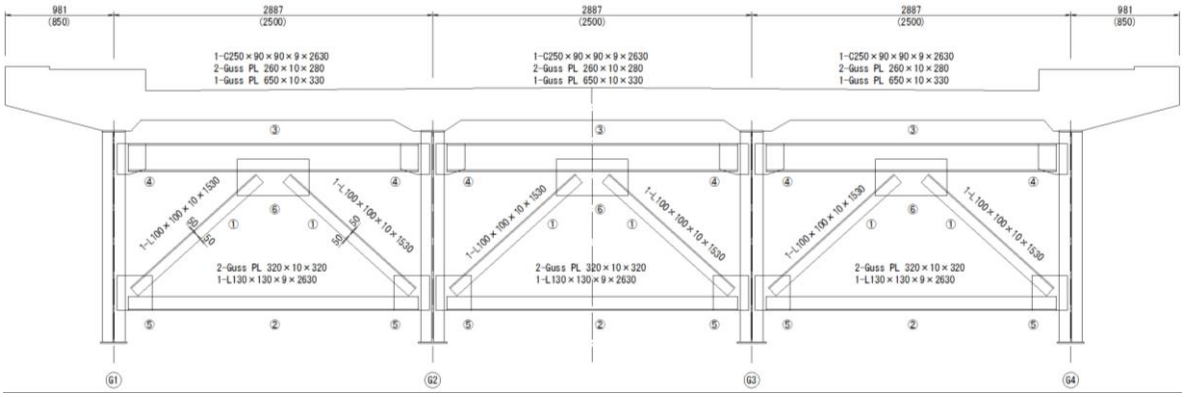


**Figure 3.1: Cross section of Hinoki bridge**

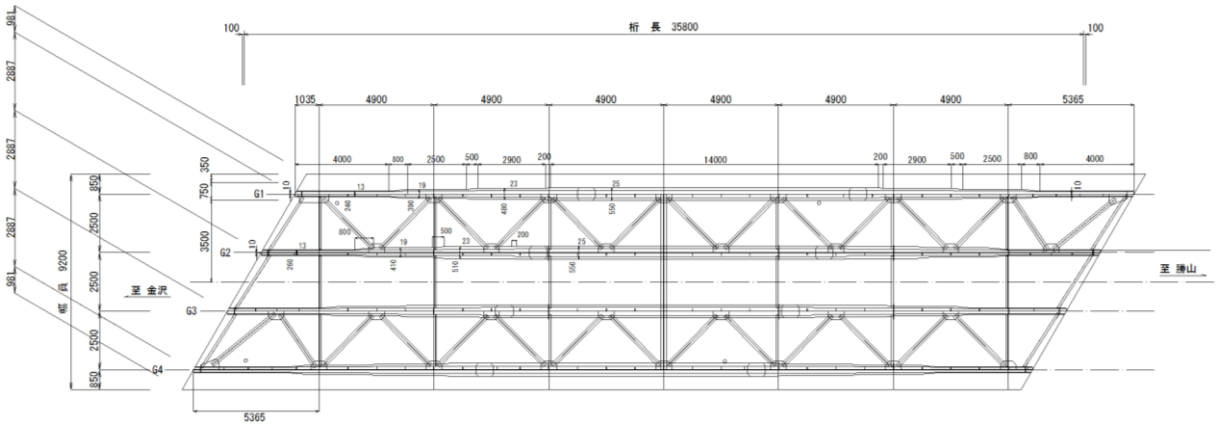


**Figure 3.2: Plane view of Hinoki bridge**

Cracked on the lower surface of the deck, white precipitate is seen. Cracks are also seen on the concrete Wheel guard surface. (Figure 3.3)

In this study, impact tests for series of rubber buffer were performed, characteristics of impact force were shown and summarized. After evaluation the bridge, depends on the reality the maintenance plans will be scheduled.

(a) Concrete wheel guard

(b) The state near the joint of bridge

**Figure 3.3: Fatigue damage of reinforce concrete on highway bridge**

Impact test was conducted on the Hinoki Bridge using SIVE, the U side was done from impact cushion Type B, falling height 15, 30 cm, D side was impact cushion Type E, falling height Impact test was conducted from 30 cm. Type B of rubber cone (rubber buffer KFDF-51, Tokyo- sokki kenkyujo co. ltd) is normal rubber, 48 mm of height, 40 mm of diameter. Type E are low rebound rubber (Hanenaito, Naigai rubber industry co. ltd.) with the height is 32 mm and the diameter are 26.09 mm. In both case the falling weight are 220 kg.

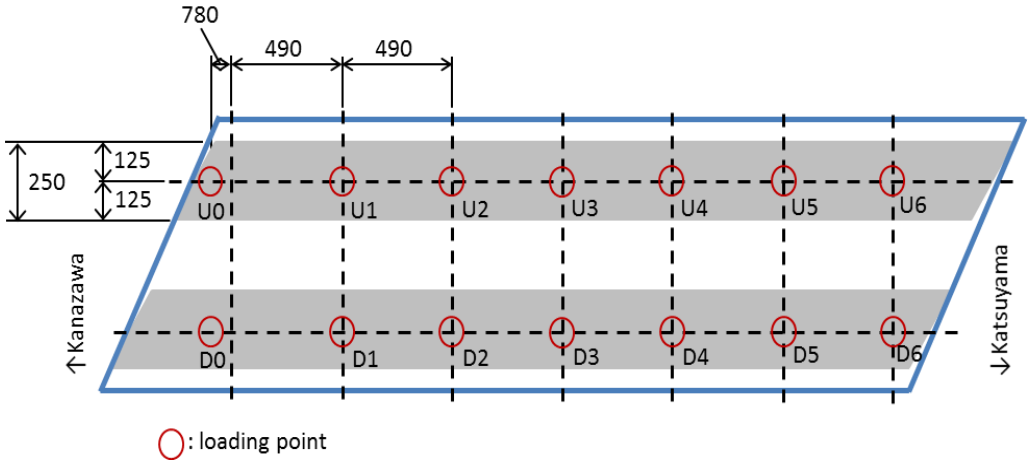


(a) loading points

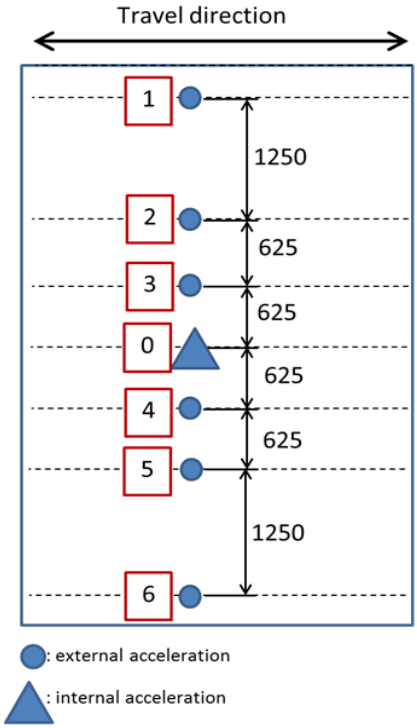


(b) Mesurement positions of acceleration

**Figure 3.4: Loading point location and External acceleration positions**

This bridge was a road with one lane on one side, and impact tests were conducted three times at each point. On the U side and the D side in the above Figure, the loading points are numbered from 0 to 6 in order from the Kanazawa direction, and the displacement meters are installed at the loading points 2 and 5 (Figure 3.4(a)). Also, the external acceleration meter was set from 1 to 6 on the U side and D side excluding the load point from the right side in the direction of travel as in the Figure 3.4(b).

(a) Loading point D2 (b) Loading point U0

**Figure 3.5: The under surface of bridge**

This time, we focused on each loading point of the bridge and organized the data. In addition, another displacement measure method was applied such as: FWD light (Figure 3.6(b)) using displacement gauges and Doppler system measure (Figure 3.6(c)) for more reference results.

(a) SIVE

(b) FWD light

(a) Laze displacement meter under the bridge

**Figure 3.6: SIVE, FWD light and Doppler system**

### 3.1.2 Experiment results

After experiment, all the data were collected and analyzed, the following example of one case results with loading point D2 and the falling height is 30 cm.

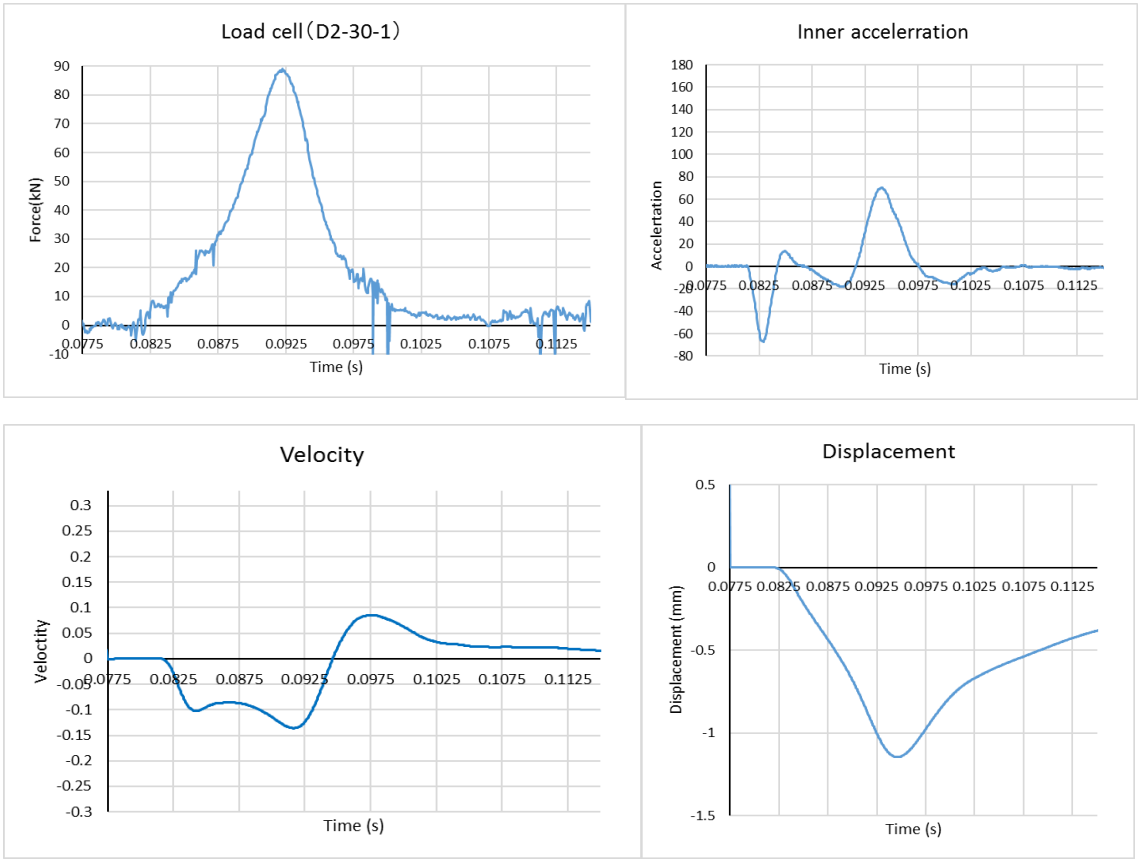


**Figure 3.7: Example of impact force, acceleration, velocity and displacement point D2**

Figure 3.7 shows the time course impact force from 0.3 height in case of loading point D2. The first impact is the most important for the dynamic behavior of structure. In this case of experiment, the impact force reached almost 90 kN in 0.025 s. In addition, the acceleration of the impact loading point, the velocity and the displacement are shown respectively. The velocity and the displacement were numerically integrated once and twice from the acceleration. To avoid damage to the pavement by impact, thin soft rubber sheet was laid on the pavement under impact point. Since a relatively large displacement including the displacement of rubber was observed at the striking point, the interpolation was performed for only the central displacement using the other four displacements

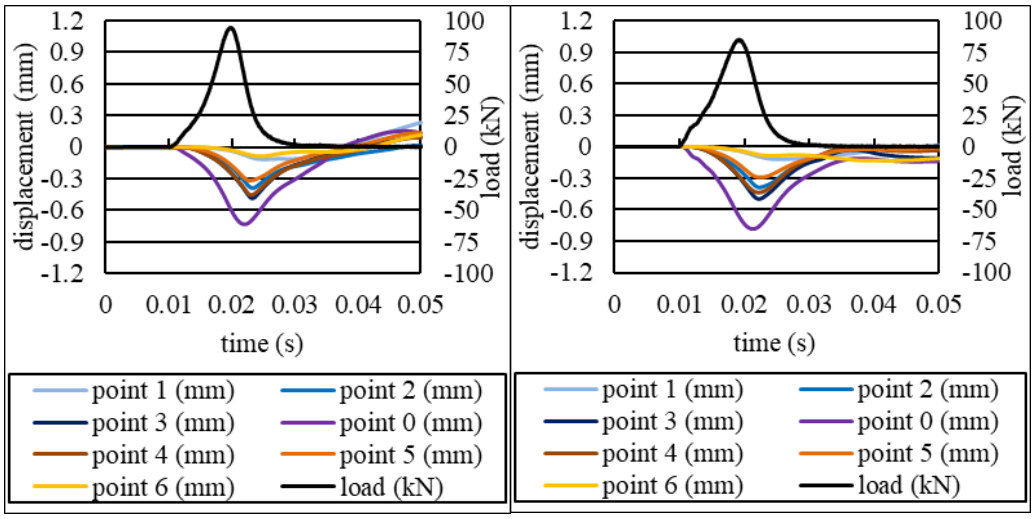


(a) Loading point D1 (b) loading point D3

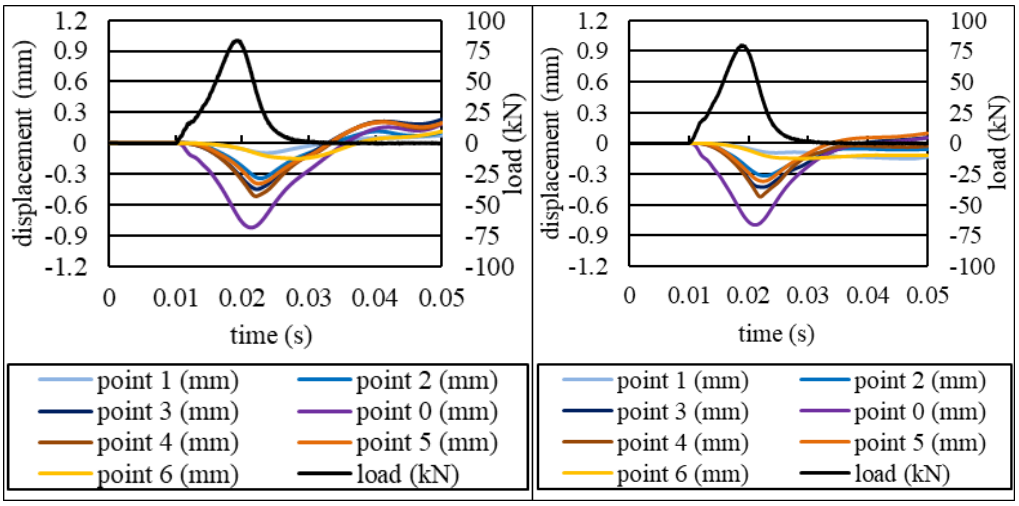


(c) Loading point U1 (d) Loading point U4

**Figure 3.8: Load and displacement of all point at loading time**

The figures below show the loading point displacement and the calculated displacement from the external accelerometers 1 to 6 at the time when the loading point displacement became the maximum, and the numbers on the horizontal axis. In the impact test of this time, it is estimated that the Hinoki Bridge itself was old, the degradation of asphalt was advanced due to the traffic load etc. It is assumed that the impact point was displaced more than originally at the point of loading. Also, in order to suppress the shock at the time of loading It is thought that 1 cm rubber is also a cause of large deflection. To predict displacement originally obtained, we decided to displace at the loading point by using shape function from external acceleration. After

correction by the shape function, the integral displacement (amount of deflection) obtained at the loading point was a value estimated from the amount of deflection at external accelerations 1 to 6.

5 → loading point

1 → external accelerometer 1

3 → external accelerometer 2

4 → external accelerometer 3

6 → external accelerometer 4

9 → external accelerometer 6

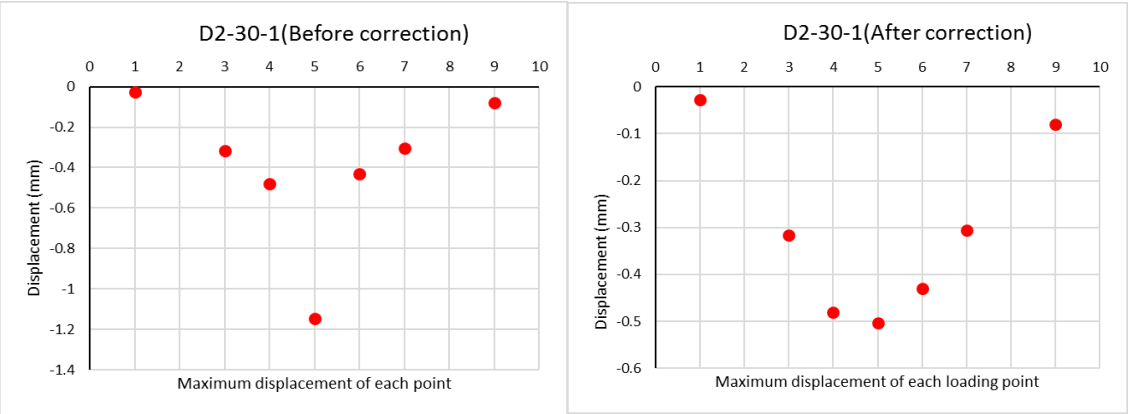


(a) (b)

**Figure 3.9: Maximum displacement of loading point D2 before and after correction.**

Figure 3.9 (a) shows the maximum value of displacement in each point of external and inner acceleration. However, the results seem to have the phenomenal differences between the value of loading point and external point. Looking at these plots, we can see that the calculation displacement at the loading point is large. What is considered as a cause is that the asphalt pavement has been damaged due to the damage condition. Therefore, based on the calculated displacement obtained from the external

accelerometer, the displacement of the actual bridge deck slab is considered by using the shape function. Using interpolation method for approximating between values of a given function and handling it as a continuous function.

Interpolation method called shape function is widely used for approximation of continuous displacement field in element in finite element method. If a certain finite element has n nodes and its shape function is Ni (i = 1, ..., n), Ni is expressed as at node i= 1, the other node is 0. It is defined as a continuous function having the property that when the shape function is used, the function value of the element is always

$$\sum_{i=1}^{n}(\boldsymbol{Node\ i\ value}) \cdot \boldsymbol{N_i} \qquad \textbf{(3.1)}$$

The function values $y_1$, $y_2$,……., $y_n$ at nodes, the shape function is

$$\{\boldsymbol{y}\} = \begin{Bmatrix} \boldsymbol{y_1} \\ \boldsymbol{y_2} \\ \vdots \\ \boldsymbol{y_n} \end{Bmatrix}, \{\boldsymbol{N}\} = \begin{Bmatrix} \boldsymbol{N_1} \\ \boldsymbol{N_2} \\ \vdots \\ \boldsymbol{N_n} \end{Bmatrix} \qquad \textbf{(3.2)}$$

When the vector display with the function $\{\boldsymbol{y}\}^{\boldsymbol{T}} \cdot \{\boldsymbol{N}\}$

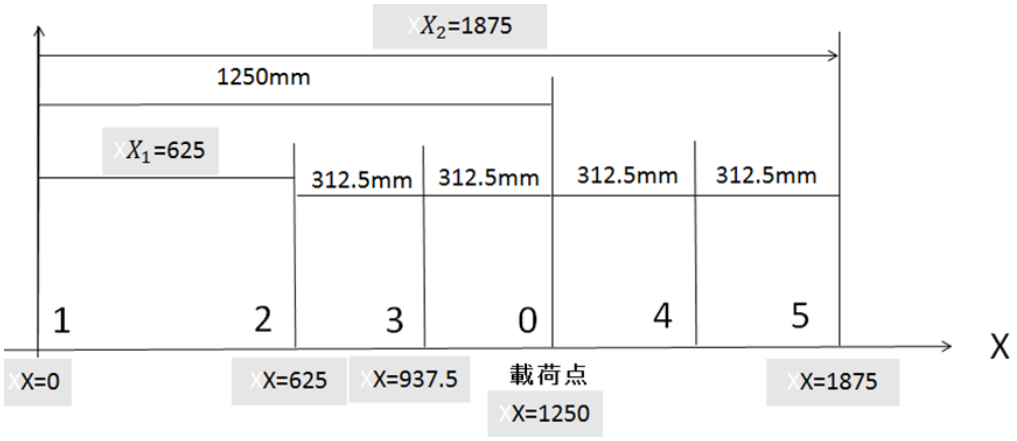


**Figure 3.10: Interpolation method**

After the calculation of shape function, the results was show in Figure 3.11. The same methods were done for all the loading point.

Figure 3.11 shows the maximum displacement of each point with the data collected by external accelerations. The falling heights are 15 cm and 30 cm respectively. The maximum displacement are about 0.24 mm and 0.49 mm respectively. It can be seen that the displacement is proportional to the energy of weight.

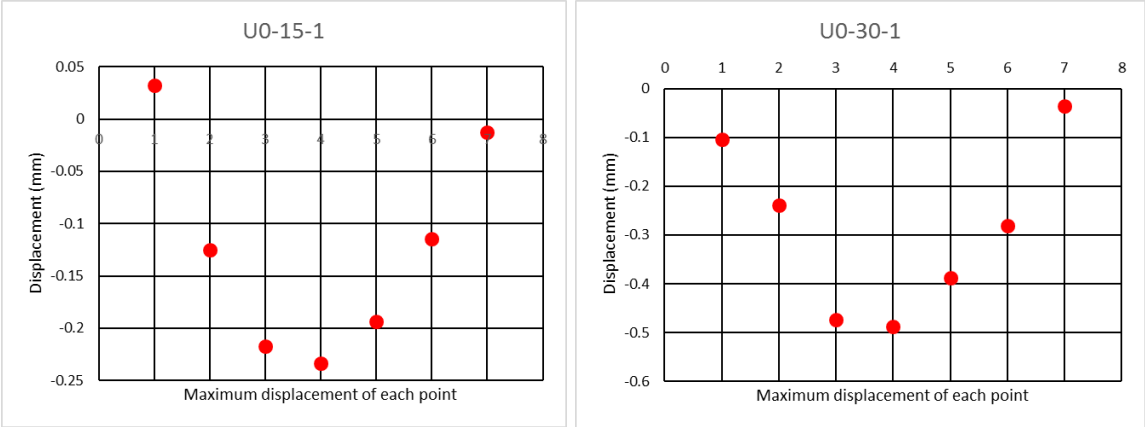


**Figure 3.11 Maximum displacement of point U0 on U side**

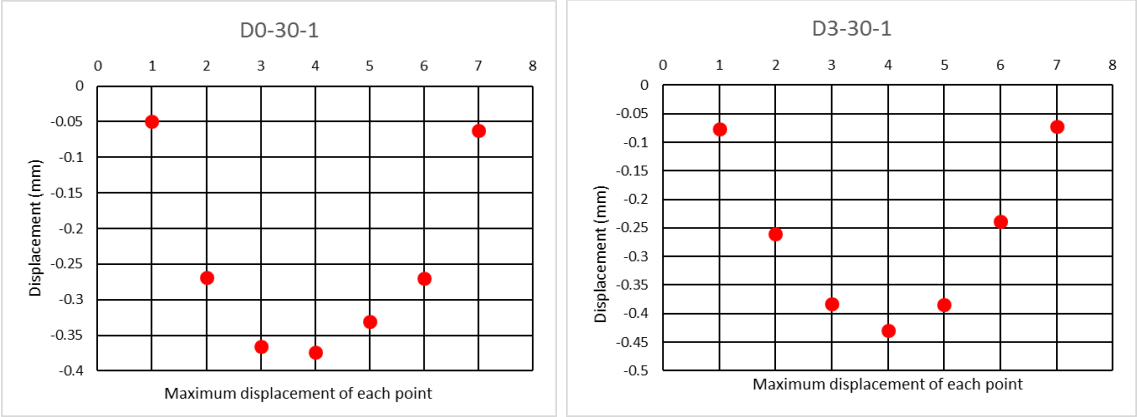


**Figure 3.12: Maximum displacement of the point D0 and the point D3 on D side**

Figure 3.12 shows the results of displacement on D side, the point D0 and the point D3. It can be seen that the maximum displacement in D0 and D3 are approximately 0.38 and 0.43 mm respectively. It seems that the bigger displacement was found in the loading point D3 which is in the center of the bridge slab.

Absolute displacements of all point on D side from D0 to D6 which was done three times for each point were concretely shown in Figure 3.13. The results of loading point D1, D2, D4 and D5 have almost the same value in three times. Other points

experienced the small differences. In addition, about 1.8 mm of displacement in D0 were the biggest of all point. On D side the falling height is 30 cm and the rubber cushion type 2 with the average value of maximum impact force is approximately 90 kN

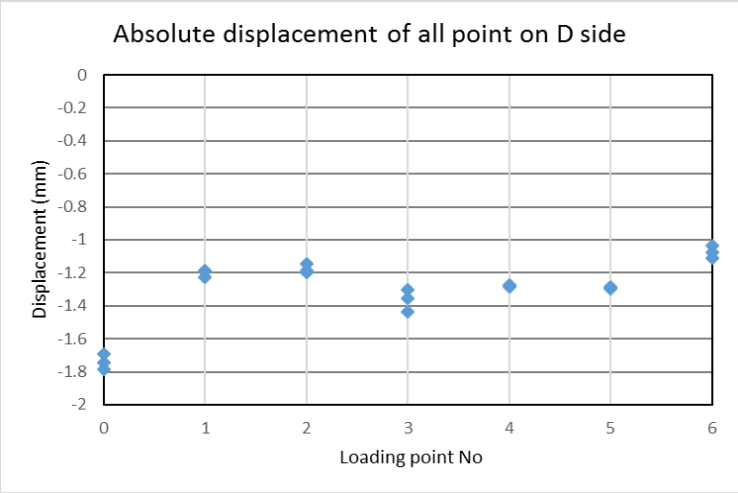


**Figure 3.13: Displacement of all point on D side with the falling high 30cm**

Figure 3.14 shows the displacements of all point on U side of Hinoki bridge in both falling height 15 cm and 30 cm. As can be seen, the displacement of U side with the 30 cm of falling height was higher than one with 15 cm and it corresponds with the energy of falling weight. The average value of maximum impact force is roughly 105 kN in case of 30 cm falling height, moreover about 45 kN is the average one in case of 15 cm falling height. On this side the experiment was done with three times of each point in both of the falling high, in Figure 10(b), the results of all point in all times were coincident. On the other hand, loading point U2, U3, U5 and U6 in Figure 3.14(a) had quite various value in three times of test. As can be seen, the largest value of displacement are approximately 1 mm and 1.55 mm for falling height 15 cm and 30 cm respectively. In this side with the normal rubber cushion type 1, the maximum impact force was increased more than twice in case 30 cm than in case 15 cm of falling height. However, the differences of displacement did not seem to be double

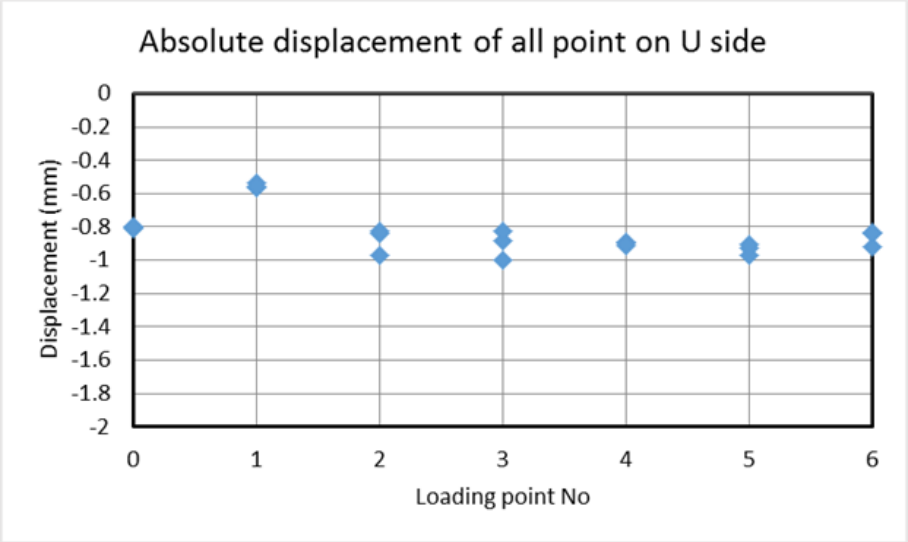


(a) Displacement of all point on U side with the falling high 15 cm

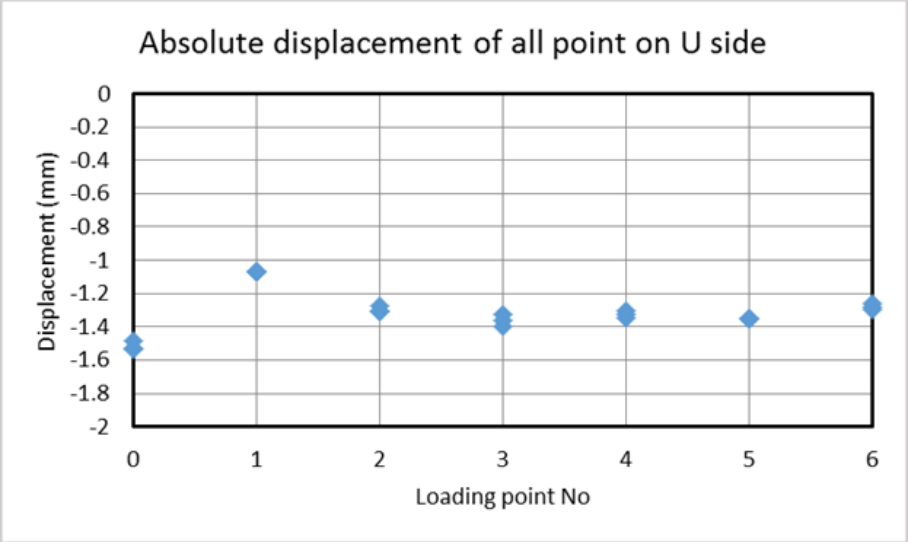


(b) Displacement of all point on U side with the falling high 30 cm

**Figure 3.14: Absolute displacements of all point**

### 3.1.3 Comparison of displacements

In this experiment other system was used, FWD light with the height of falling was 110 cm with the average maximum of impact force are roughly 18 kN and 17 kN on D side and U side respectively. On D side the maximum displacement value is approximately 1.2 mm in point D3, by this system the data were collected in various numbers. The same trend was seen on the results on U side. Each time of test has a difference. Furthermore, the values of SIVE were larger than those of FWD light.

Comparing with the results of SIVE, Figure 3.15(a) shows the largest value of displacement by FWD light was about 1.2 mm while it was roughly 1.55 mm

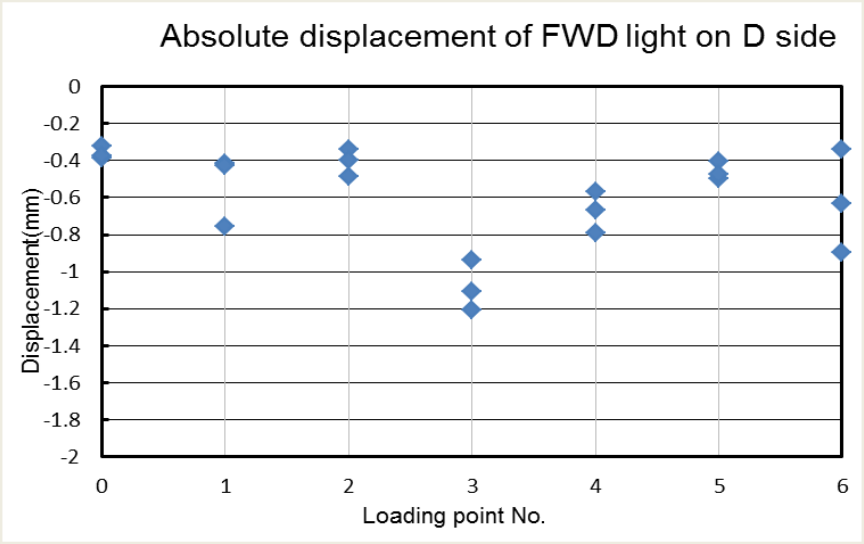


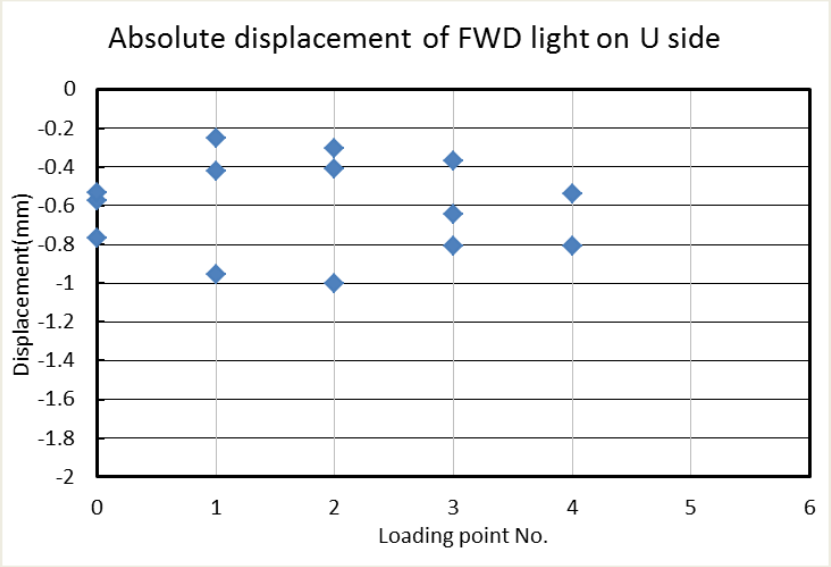


**Figure 3.15: FWD light displacements results on D side and u side**

Furthermore, in Figure 3.15(b) as can be seen the maximum value of displacement on U side by FWD light was equivalent with the results of loading point 1 and 2 by SIVE. This value was approximately 1 mm.

In brief, in this experiment on Hinoki bridge the result between SIVE and FWD light are quite comparable each other. Displacements which are collected by Doppler measure, the average values are lower than the one from SIVE. In U0 loading point we can see the large difference between the values, in addition to loading point 1 and

4 with the displacement gauges were the smallest value on U side. Whereas on D side these values seem to be in proportionate to others result such as Doppler average displacement value.

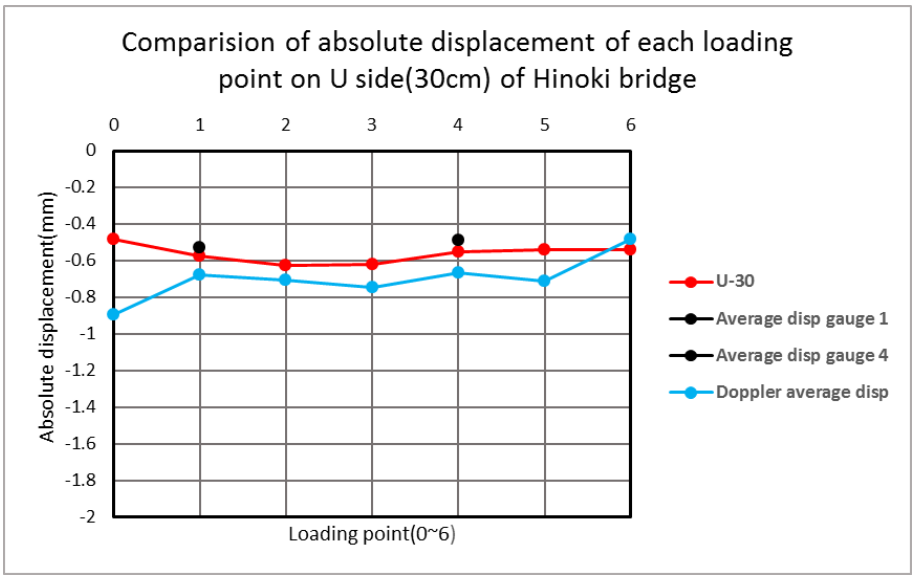


**Figure 3.16: Comparison of absolute displacement in U side (30 cm)**

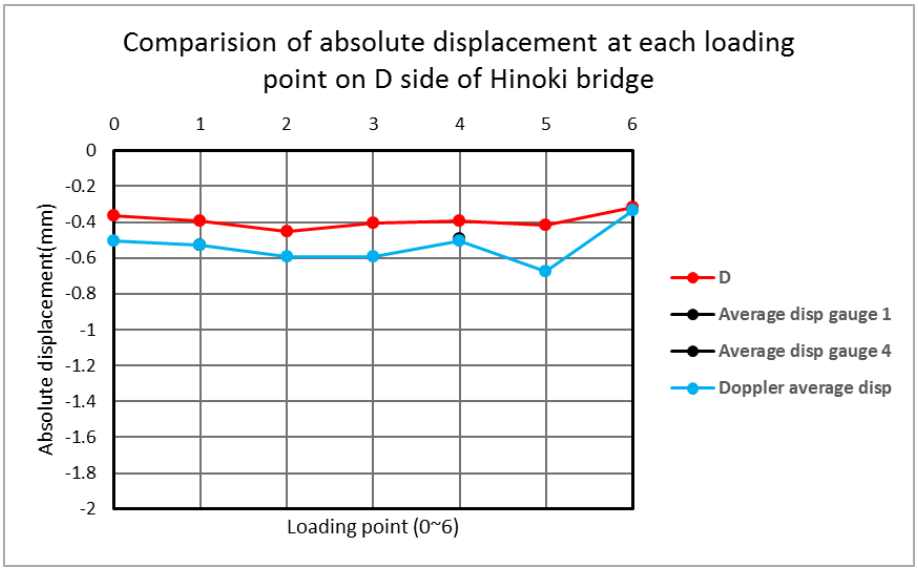


**Figure 3.17: Comparison of absolute displacement in D side (30 cm)**

In addition, on D side the same trend has been seen in the displacement values. Some positions values are diverse, in otherwise displacement gauge was almost the same values with Doppler one. As can be seen, the experiment results which are calculated from SIVE system and other displacements measure methods have the critical differences. Other investigation is now scheduled to be done in Hinoki bridge. In the

future experiments, it is important to clarify the cause of large displacement at the loading point, and it seems to lead to a smoother analysis. It is expected that the amount of displacement at the loading point has increased since the pavement of Hinoki Bridge was damaged in many places. Also, it may be thought that the deflection of the loading plate rubber (3 mm) laid in order to suppress the jump of the impact test has come out.

In the future experiments, it is important to clarify the cause of the large displacement at the loading point, and it seems to lead to a smoother deterioration evaluation.

After a series of experiments on Hinoki bridge we have some conclusion. Rubber type E which is low rebound rubber is the ideal one to control the maximum impact forces. The result of displacement which is calculated by the acceleration in SIVE are quite equivalent with the result of FWD light. Some differences were found in the results, detailed inspection and further experiments by this method are now scheduled to get more accurate results. They give concrete information on repair.

We would like to accumulate displacement data of many bridge slabs by this SIVE and build reliable and accurate checking method. We will also conduct research on analytical reproduction.

### 3.2 Yatsuo Bridge

#### 3.2.1 Experiment outline

Yatsuo Bridge, as the target of this research, is a synthetic plate girder bridge with three spans and is located on a city road in Toyama Prefecture. The bridge has five main girders, and reinforced concrete is used for the deck slab (hereinafter referred to as RC). The length of the objective span is 29.20 m, and the total width is 14.80 m. At the time of the testing, a number of places showed discoloration from water exposure on the lower surface of the slabs during a visual inspection.

Object span

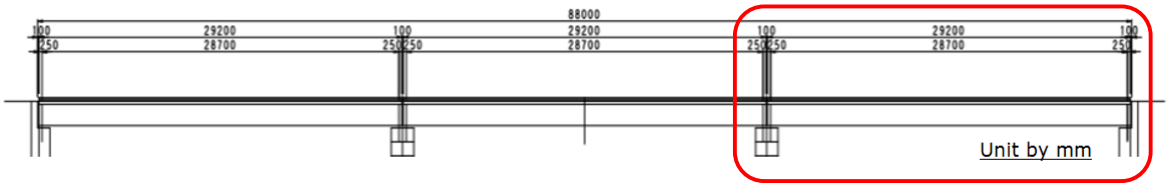


**Figure 3.18: Yatsuo Bridge**

**Figure 3.19: Deterioration of bridge deck**

Falling weight deflectometers (FWD) are fixed to a vehicle and generally used for pavement inspection [6,7]. In this research, we used SIVE, which was developed to enable a load on the bridge slabs at any position. The generated impact force is transmitted to the load board and load cell, and the load board with an area of 76,500 $mm^2$ applies the impacted force to the pavement surface of the bridge. Regarding the preliminary experiments, a low rebounding rubber with 15 rubber cones was chosen (Hanenait, Naigai Rubber Industry Co., Ltd.) The falling weight was 250 kg and the falling height was 150 mm. The load positions were set to 11 points per row, as shown in Figure 20. At the yellow loading point in the figure, a sensitive displacement gauge

(CDP-25, Tokyo Instruments Research Institute) was installed on the back of the deck slab, and the actual displacement was measured. The loading at each position was applied twice.

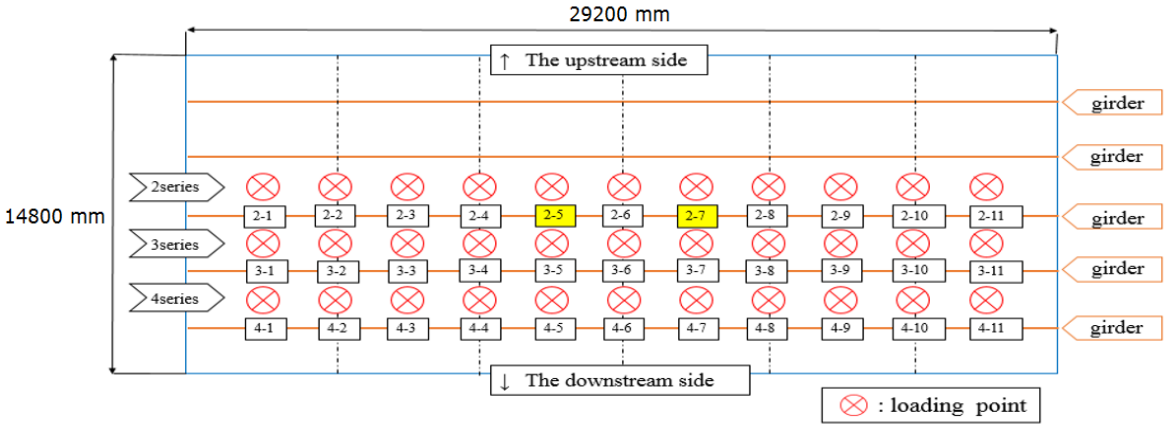


**Figure 3.20: Plane view and loading point**

The loading value was measured using a load cell provided between the loading plate and the low repulsion rubber installation plate (KCE - 500 KNA, Tokyo Instrument Research Institute). For each loading, the acceleration at each point was measured using an accelerometer (ARJ-200A, Tokyo Instruments Research Institute). Accelerometers were installed side by side in the direction of the bridge axis. The measurement positions were set to seven points in total, namely at 35 cm, 70 cm, and 140 cm on the left and right sides of the loading point. The load and acceleration were measured at 20 kHz for 0.1 s. The displacement of the accelerometer installation position was calculated by integrating the acceleration of the second order over time.

### 3.2.2 Experiment results

About impact load and loading time. On average, the maximum impact load is 49.0 kN with an impact time of 0.032 s. Figure 3.21 shows an example of the time history of the impact load. The load value for a falling weight increases dramatically over time, and decreases sharply after reaching a peak at 47.9 kN, and the duration of the impact force is 36 ms

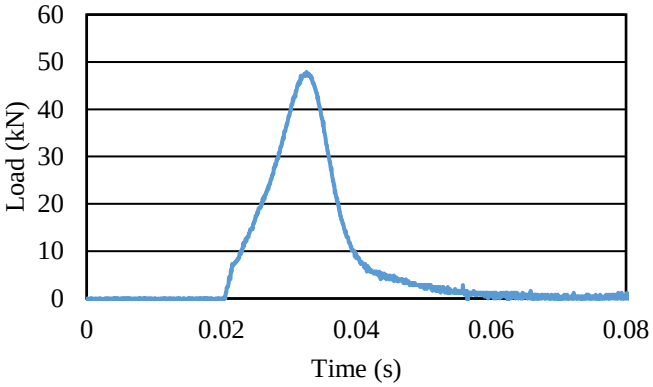


**Figure 3.21: Impact load (point 2-10)**

After experiment we collect impact load and displacement of all the point

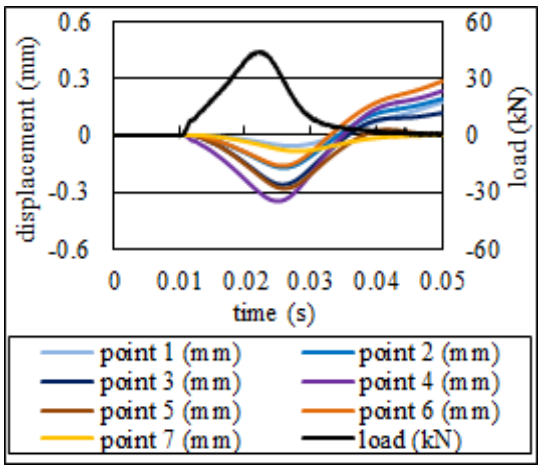


(a)

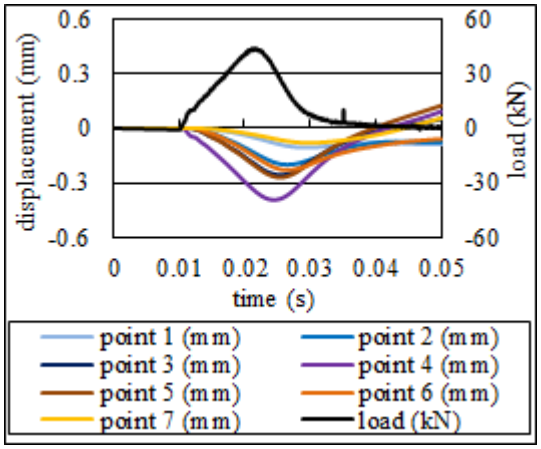


(b)

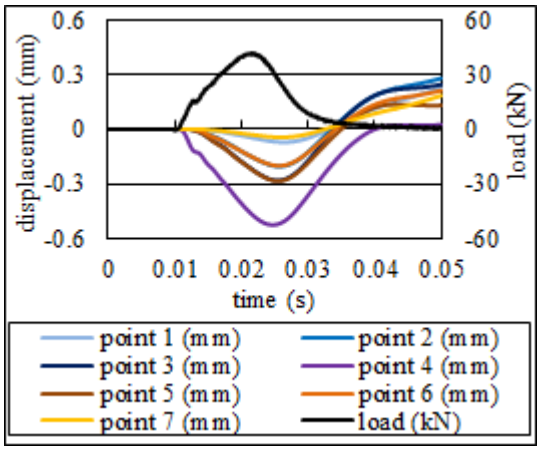


(c)

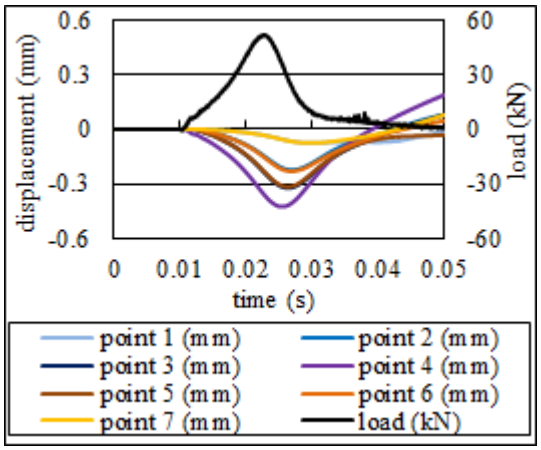


(d)

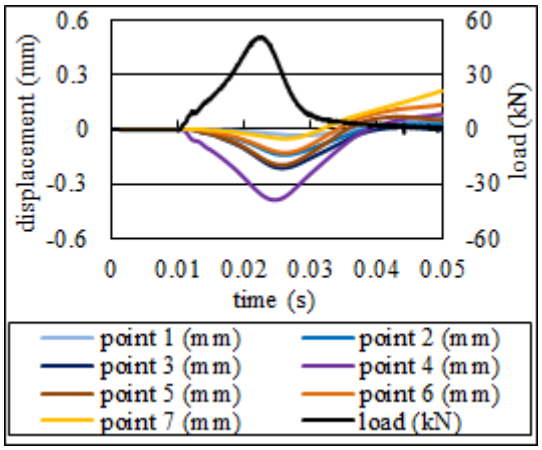


(e)

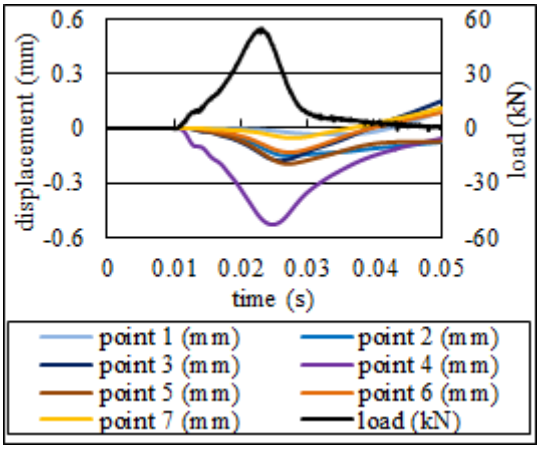


(f)

**Figure 3.22 Displacement from all accelerations**

Measurement displacement waveform by accelerometer will be described. Figures 3.22 from (a) to (f) show measured waveforms at the time of loading in the vicinity of a part of the spar end part and the center part of the span for each bridge and each panel row of point 2.1, 2.6, 3.1, 3.6, 4.1, 4.6 respectively. From these figures, it can be seen that displacement of the bridge occurs at the loading point most quickly, and thereafter displacement occurs except at the loading point. It is thought that the displacement is caused by the impact at the time of load propagating around the load point and around. Also, it can be seen that the time when the displacement at each measurement point reaches the maximum value is delayed compared to the time at which the displacement of the load point shows the maximum value.

In addition, the accelerometer is not synchronized with the Doppler displacement meter, and both waveforms do not coincide completely in terms of time. At the time of loading, it can be seen that there are measurement points where the measurement displacement by the accelerometer shows a displacement partially equivalent to the measurement displacement by the Doppler displacement gauge, but a larger value is measured. From this, the loading point displacement measured on the pavement upper surface tends to be larger than that measured on the lower surface of the deck. In the experiment, the magnitude of the displacement is measured at a predetermined point at the time of loading. Therefore, it is possible to express the displacement distribution. Here, the displacement distribution between the digits at the time when the loading point becomes the maximum will be described.

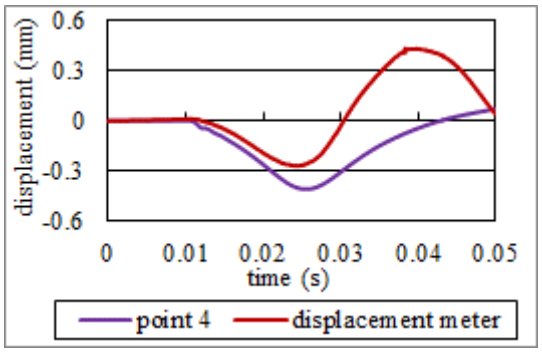


Point 2-5

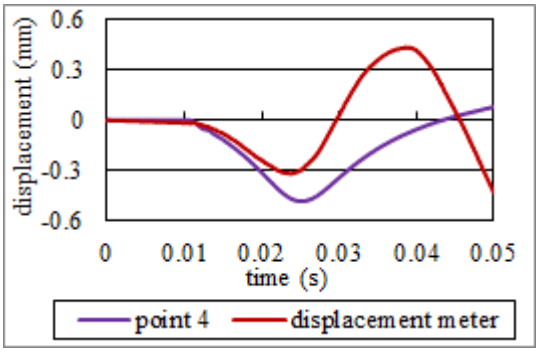


Point 2-7

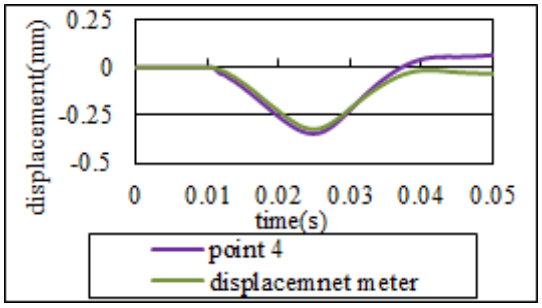


Point 2-1, Doppler displacement

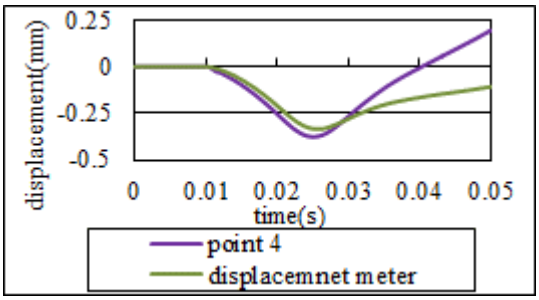


Point 2-3, Doppler displacement

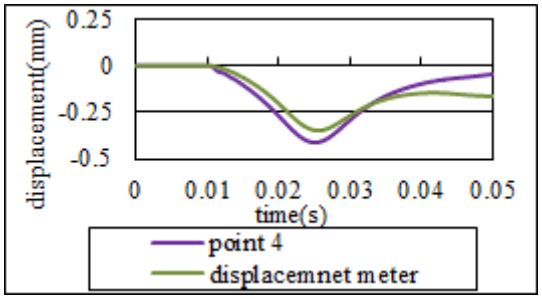


Point 2-6, Doppler displacement

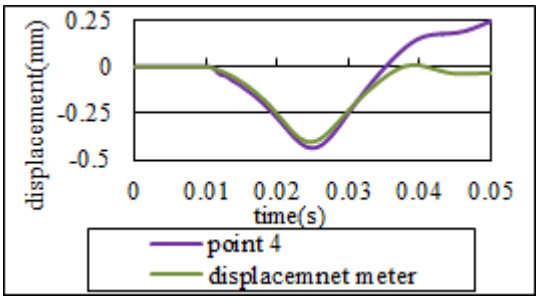


Point 2-11, Doppler displacement

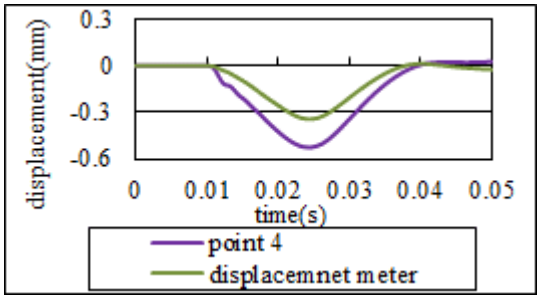


Point 3-1, Doppler displacement

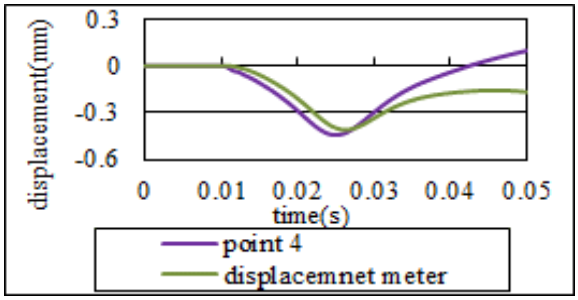


Point 3-6, Doppler displacement

**Figure 3.23 Displacements by SIVE, Displacement gauges and Doppler system**

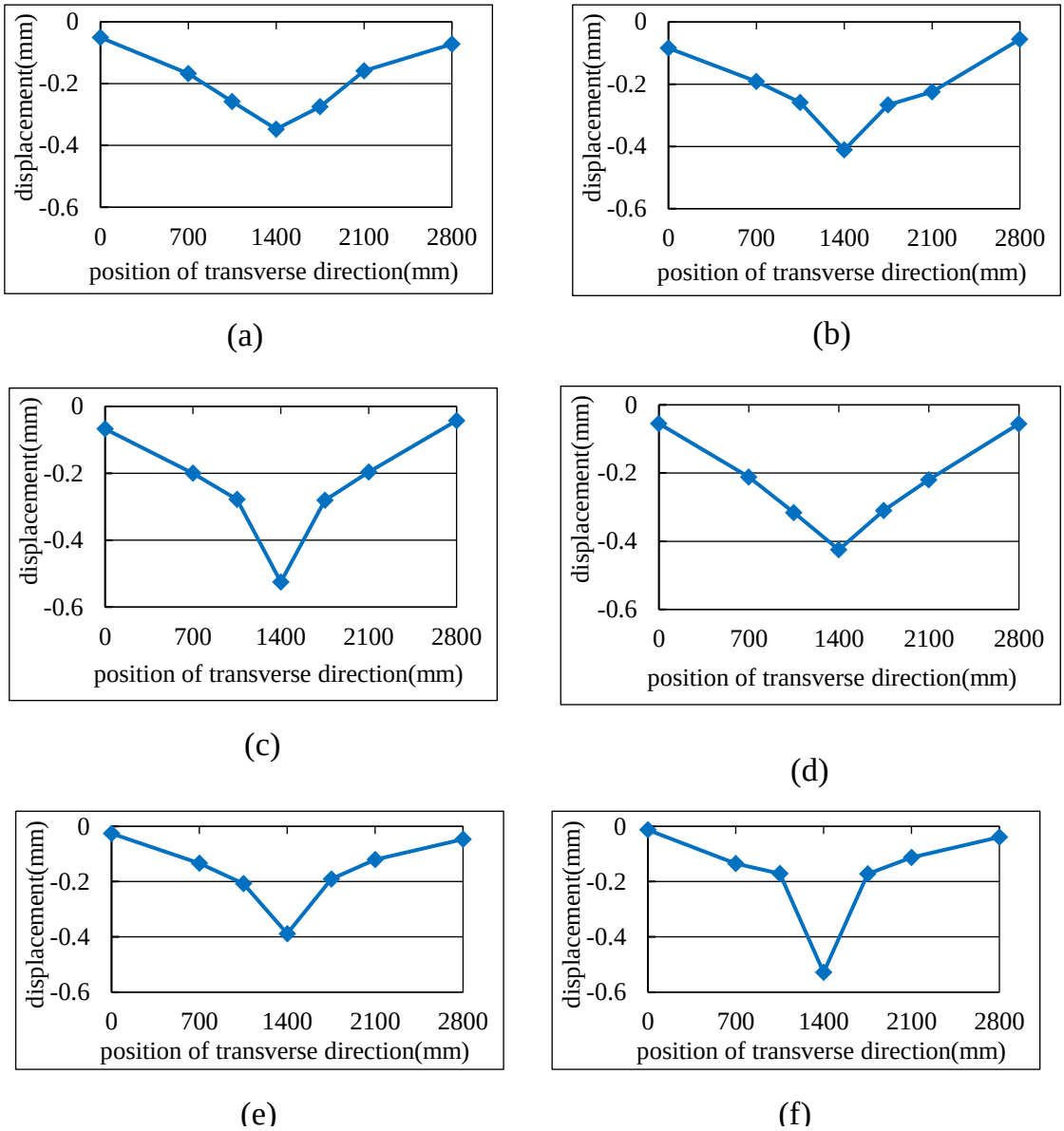


**Figure 3.24 Displacement distribution**

Figures 3.24 show the displacement distributions of some spar ends and span central positions in series line. These graphs show that the displacement distribution at points other than the loading point shows a shape that is relatively smooth, whereas the displacement of the loading point shows a sharp shape. However, observing the actual bridge floor slab, since damage such as punching and breaking cannot be found anywhere, it is considered that this is not in conformity with the actual displacement of the deck. Moreover, since the displacement distribution is measured indirectly from the pavement rather than the direct displacement of the floor slab, it may be considered that it may be influenced by the pavement.

The results of points 2–5 (Figure 3.25) and 2–7 (Figure 3.26), where displacement meters were installed, are examples of each loading test applied. The average values after conducting the test twice for each point are used in the graphs. The upward displacement has a positive value, and the downward displacement has a negative value, which appear when the loading point is at the maximum displacement. The points at 0 and 2900 mm are girders, and the points at 1,450 mm are loading positions. From Figures 3.24 and 3.25, it is shown that the displacements at the loading point are larger than the results from the displacement meter on the lower surface

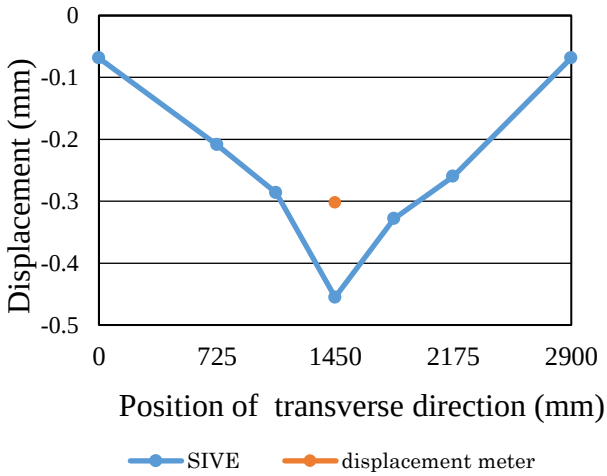


**Figure 3.25: Displacement distribution of points 2–5**

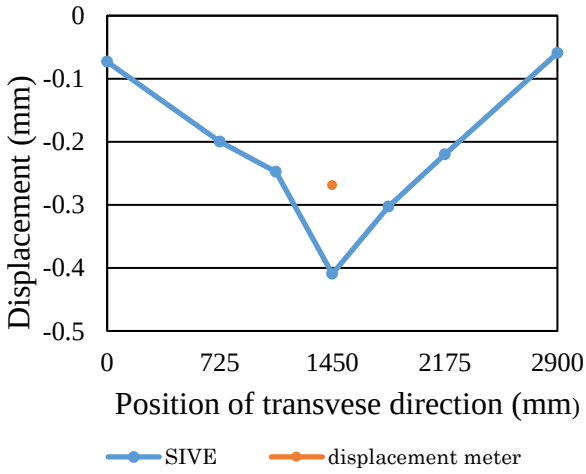


**Figure 3.26: Displacement distribution of points 2–7**

The differences between the values of the displacement meter on the lower surface of the slab and the measured displacements are large. The displacement of the loading

point is thought to be significantly influenced by the pavement. Therefore, the results of the loading point displacement based on Newton's interpolation are shown in Figure 3.27. The interpolation value was almost the same as the displacement obtained from the displacement meter at the position where the displacement meter was installed.

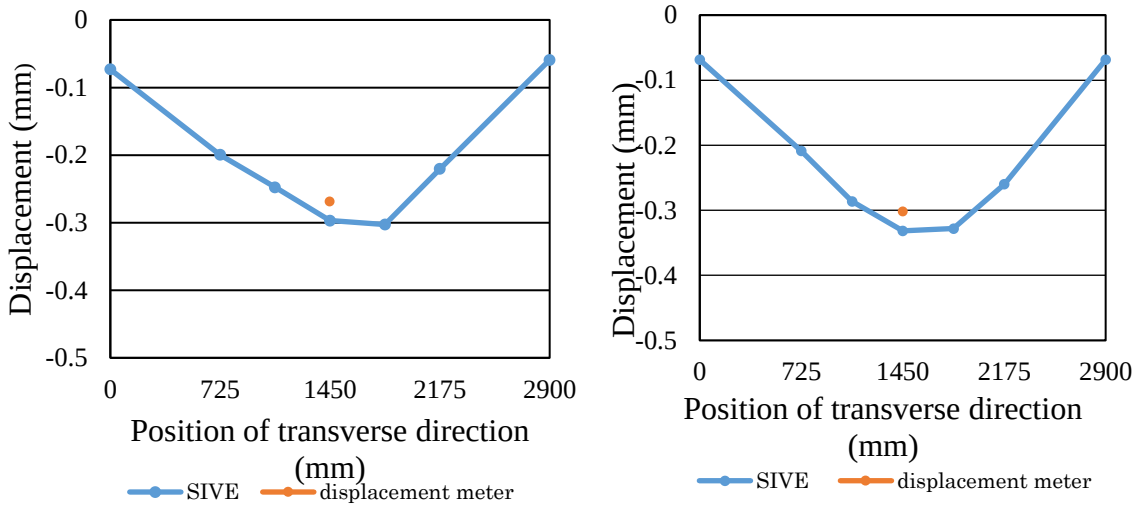


**Figure 3.27: Displacement distributions after Newton interpolation of points 2–5 and 2–7**

It is clearly that, the displacement of the loading point was influenced by the pavement, after use interpolation, the results quite equivalent with the displacement meter. Other points of SIVE loading test experienced the same trend with Doppler system and displacement gauges which were installed on lower surface.

## References

[1] Japan road association: Design specifications for steel highway bridges/Production specifications for steel highway bridge, Gihoudo Co. Ltd., 1956.

[2] Japan road association: Specifications for highway bridges part2 steel bridges ver. 2002, Maruzen Co. Ltd., 2002.

[3] Masuya, H., Yokoyama, H., Sekiguchi, M., and Xu, C. (2015). "Study on impact behavior of fatigue deteriorated reinforced concrete slab by finite element method" Proceedings of 11th International Conference on Shock & Impact Loads on Structures, 267-272.

[4] Nguyen, T. N., Masuya, H., Xu, C., Kaii, H., Yamaguchi. T., and Yokoyama, H. (2016). "Self-propelled impact vibration equipment for the ultilization of inspection of bridge deck" Proceedings of 9th Symposium on Decks of Highway bridge

[5] Japan Road Construction Association: FWD (Pavement Structure Evaluation Equipment), Japan Road Construction Association, www.dohkenkyo.net/pavement/kikai/fwd.html (browsing date: January 6, 2018)

[6] Abe Nagato, Maruyama Takahiko, Himen Kenji, Hayashi Masanori: Structural Evaluation of Pavement based on Deflection Evaluation Index, Papers of the Japan Society of Civil Engineers, Vol.18, No 460, pp. 41–48, 1993.

[7] Mikio Sekiguchi, Katsuro Koufu: Investigation of the Soundness Evaluation Method of the deck by FWD, Papers of Structural Engineering Vol. 50A, pp. 697–706, 2003.

[8] Yamaguchi Kyohei, Hayasaka Yohei, Soda Nobuo, Onishi Hiroshi: A proposal on Soundness Evaluation Method of Existing RC Deck using FWD, Papers of Structural Engineering, Vol. 61 A, pp. 1062–1072, 2015

[9] Hiroshi Masuya, Hiroshi Yokoyama, Chen Xu, Saiji Fukada, Yoshimori Kubo: The Development of Self-propelled Falling Weight Deflectometer Equipment for the Evaluation of the Deterioration Degree of Bridge Slab, Proceedings of 14th

East Asia-Pacific Conference on Structural Engineering and Construction, CD-ROM, Ho Chi Minh City, Vietnam, 2016.

[10] Nga Thu Nguyen, Hiroshi Masuya, Chen Xu, Hiromitsu Kall, Takafumi Yamaguchi, Hiroshi Yokoyama: Self-propelled Impact Vibration Equipment for the Utilization of Inspection of Bridge Deck, Proceeding of 9th Symposium on Decks of Highway Bridge, pp. 89–92, 2016

[11] Matsumoto Daijiro, Nakamura Kazuhiro, Sato Masakazu, Kamiya Keizo: Research on Material Constants used for Repair Design of Asphalt Pavement on Expressway, Papers of the Japan Society of Civil Engineers E1 (Pavement Engineering), Vol. 69, No. 3 (Paving Engineering Paper Vol. 18), pp 1-101, 1-108, 2013.

# Chapter 4: Analysis using Finite Element Method

In the impact loading test described above, occurrence displacement of the floor slab by impact loading was measured. In this study, we estimate the degree of deterioration of the deck from these measured values also estimate the degradation degree by comparison with the analysis displacement by the impact analysis model reproducing the actual experiment situation. In this chapter, we will describe the method and results of the analysis. Also, from the actual test results described above, the measurement displacement by the accelerometer with respect to the load point shows a tendency to be larger than the measurement displacement by the gauge and the Doppler system, the displacement distribution showed a sharp shape, we also analyze the purpose of clarifying the cause of this.

## 4.1 Hinoki bridge

### 4.1.1 Analysis method

Modelling method of the target bridge in this study has two types: Solid partial model and Shell full bridge model were created

In the solid partial model, in order to reproduce the state close to the actual bridge and investigate the behavior of one panel of the slab, the floor plate and the pavement of the entire objective bridge were reproduced by the solid element. An example of this model is shown in Figure 4.1

For this type of model, we will describe details of what we created. All creation models are shown in the figure.

The Hinoki Bridge carries out the loading test only on the central part of each floor panel, and the panel is surrounded by steel girder and diagonal only, and it is surrounded by steel girder, diagonal, horizontal cross. Since there are two patterns of things, the model created two types shown in Figure 4.2.

Shell full bridge model is a one-bridge whole reproduction model in which the floor plate and the pavement are reproduced by shell elements in order to investigate the tendency of the floor slab and spar displacement due to span direction position. This

shell full bridge model is shown in Figure 4.3. In this research, we made shell bridge model only for Hinoki Bridge

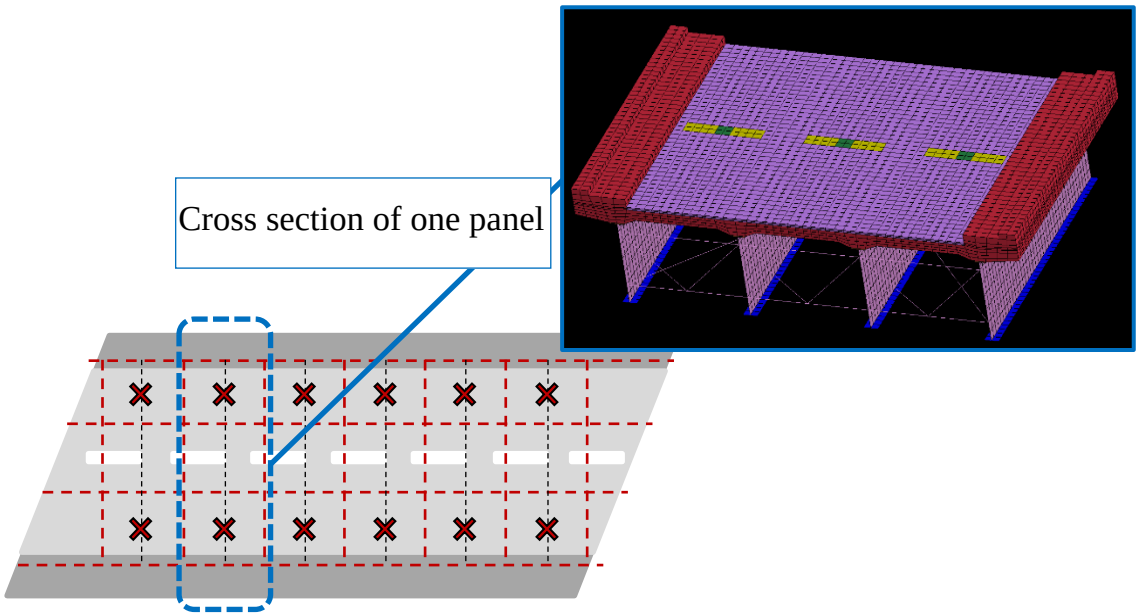


**Figure 4.1: Solid partial model**

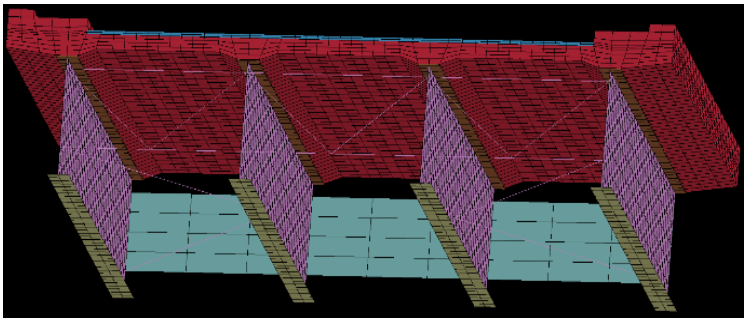

Surround by stell girder,diagonal and cross beam

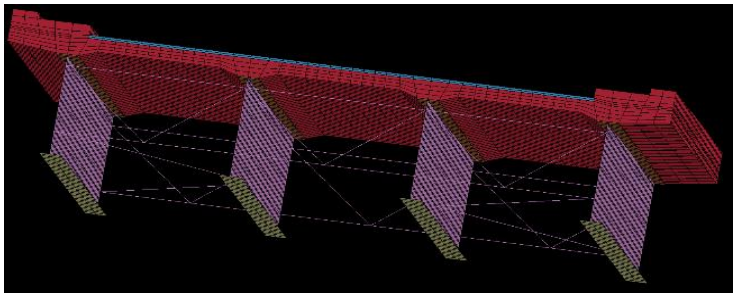

Steel girder surrounded by diagonal

**Figure 4.2: Model of one panel**

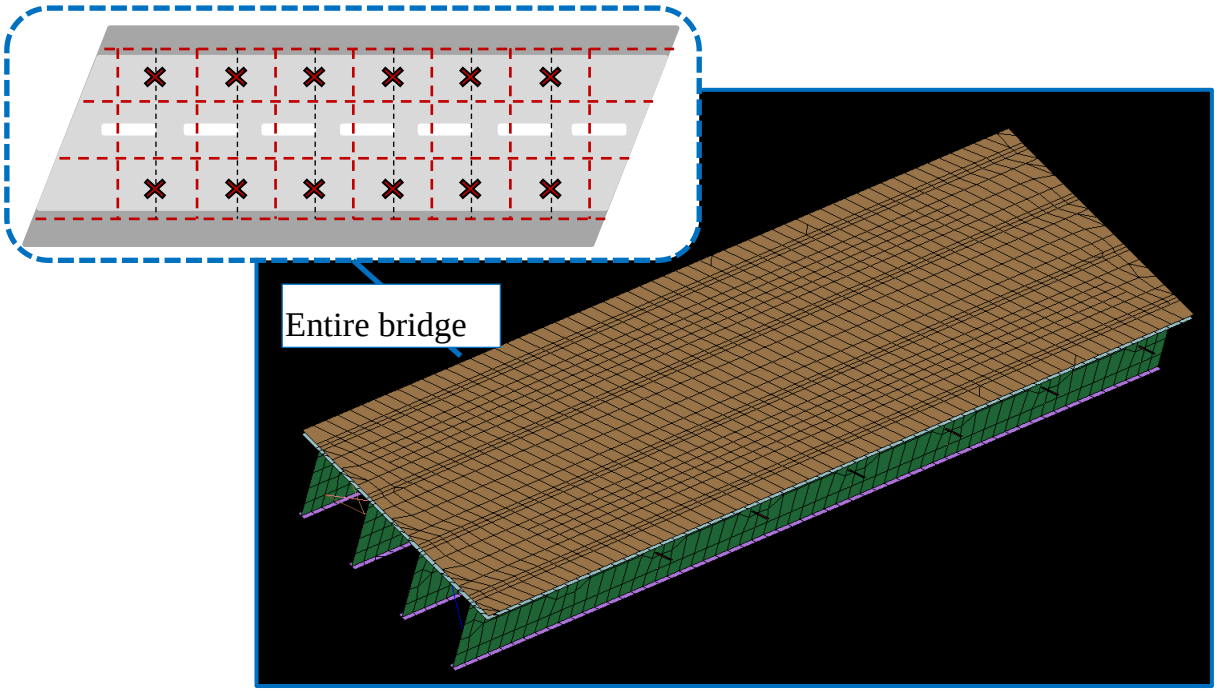


**Figure 4.3: Shell model of full bridge**

Details of the elements used for each model are shown in Table 4.1.

**Table 4.1: Details of element used in model**

| Element | | Solid partial model | Shell full bridge model |
|---|---|---|---|
| Slab | | Solid | Shell |
| Pavement | | Solid | Shell |
| Steel main girder | upper flange | Solid | Shell |
| | web | Solid | Shell |
| | Lower flange | Solid | Shell |
| Steel cross girder | | Solid | Shell |
| Truss | | truss | truss |

### 4.1.2 Analysis model

Properties of each member used for analysis here are shown in Table 4.2. All the properties were elastic and MAT_elastic was applied.

In order to examine the influence of the pavement on the displacement of the deck by the temperature change, the elastic modulus of the pavement varies with the

temperature of the outside conditions. For the cases where the temperature is 5 ° C, 15 ° C, 40 ° C respectively, the elastic modulus of the pavement is modelled.

Although the deck is required to be illustrated in each case when it is healthy and the deterioration phenomenon is hardly observed and when it is not healthy where deterioration phenomenon is observed in the case of using a floor plate as an elastic body in past research, a floor with deterioration. Since there is a case where the degree of deterioration is judged by expressing the state of the slab by the value of the converted elastic modulus, with reference to this, in this research it is assumed to assume the degradation state of the deck by changing the value of the elastic coefficient. As a specific state of the deck,

· When the target bridge is relatively healthy ($E_c$ = 21.5 kN /$mm^2$)

· When a slight degradation phenomenon such as cracks can be confirmed on the lower side (tension side) of the deck

(n = 15, ($E_c$ = 13.3 kN /$mm^2$)

· Severe degradation phenomena such as water leakage, sedimentation, horizontal cracking can be confirmed

(n = 30, ($E_c$ = 6.67 kN /$mm^2$)

Analysis was conducted for each case.

**Table 4.2: Properties of model element**

| Model element name | | Elastic coefficient (kN/mm²) | Poission's ratio | Remarks |
|---|---|---|---|---|
| Slab | Healthy condition | 21.5 | 0.2 | By the core test result of healthy part of bridge |
| | Some deterioration | 13.3 | 0.2 | At the time a relatively minor deterioration phenomenon confirmation |
| | Serve deterioration | 6.67 | 0.2 | When comparatively severe degradation phenomenon is confirmed |
| Pavement | 5℃ | 10 | 0.35 | Using reference |
| | 15℃ | 7 | 0.35 | Using reference |
| | 40℃ | 0.938 | 0.35 | Using reference |
| Steel main girder | | 200 | 0.3 | Using general value |
| Steel cross girder | | 200 | 0.3 | Using general value |
| Truss | | 200 | 0.3 | Using general value |

Contact conditions and boundary conditions are shown in Figures 4.4 and 4.5.

For both models, contact of each member was set based on node sharing. However, regarding the contact between the deck and the pavement in the shell model, it is considered that the displacement of the pavement may influence the displacement

measurement value as compared with the actual test, so that the positional relationship between the deck and the pavement is considered.

Both models were applied to the lower flange of the main girder. In the solid partial model, displacement restraint in the horizontal two directions and in the vertical direction was applied to the girder end portion, and displacement restraint in the vertical direction was applied to the entire lower flange portion other than the end portion. The shell model applied displacement restraint in the horizontal two directions and vertical direction to the girder end according to the actual installation situation.

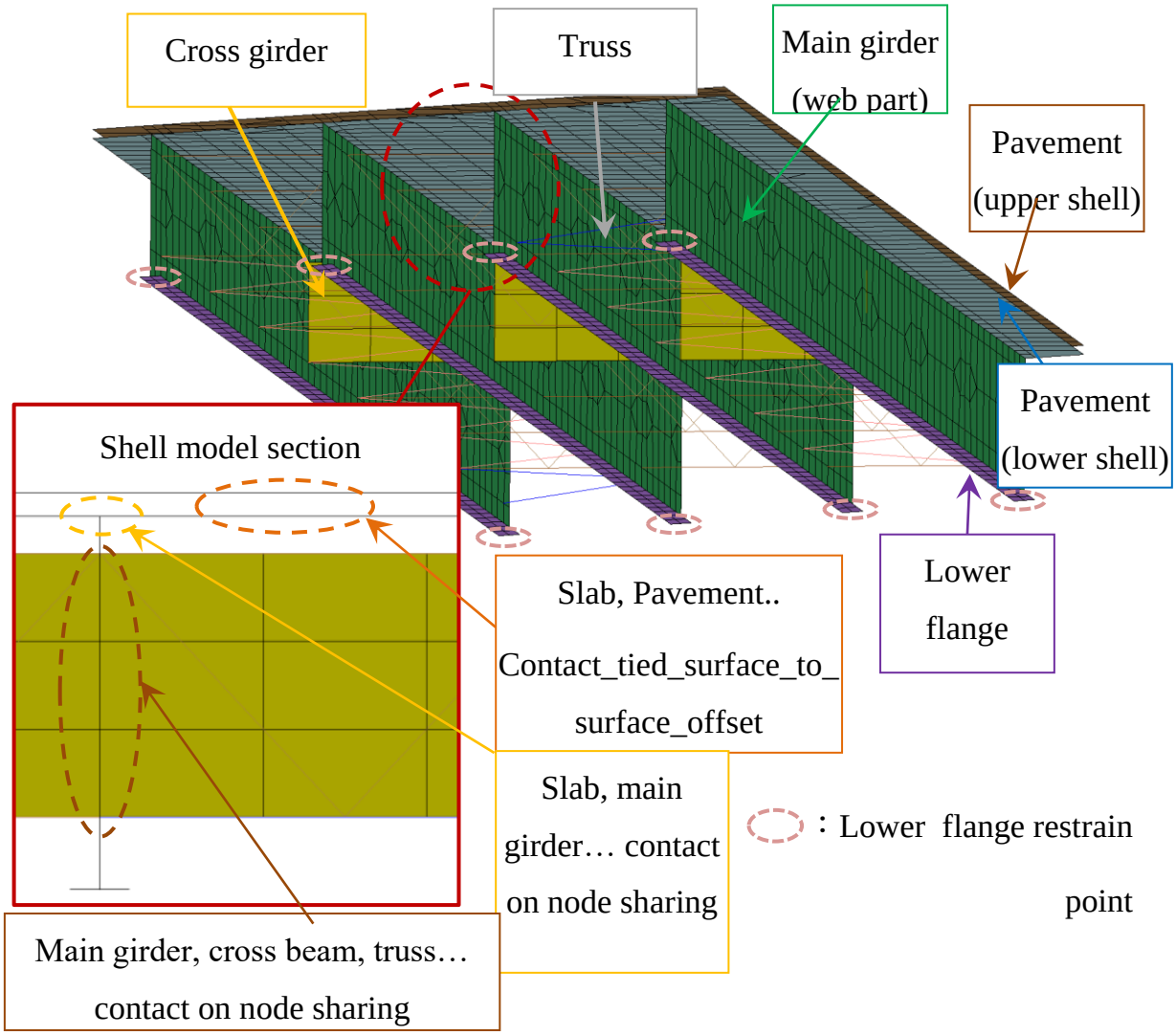


**Figure 4.4: Shell full bridge model**

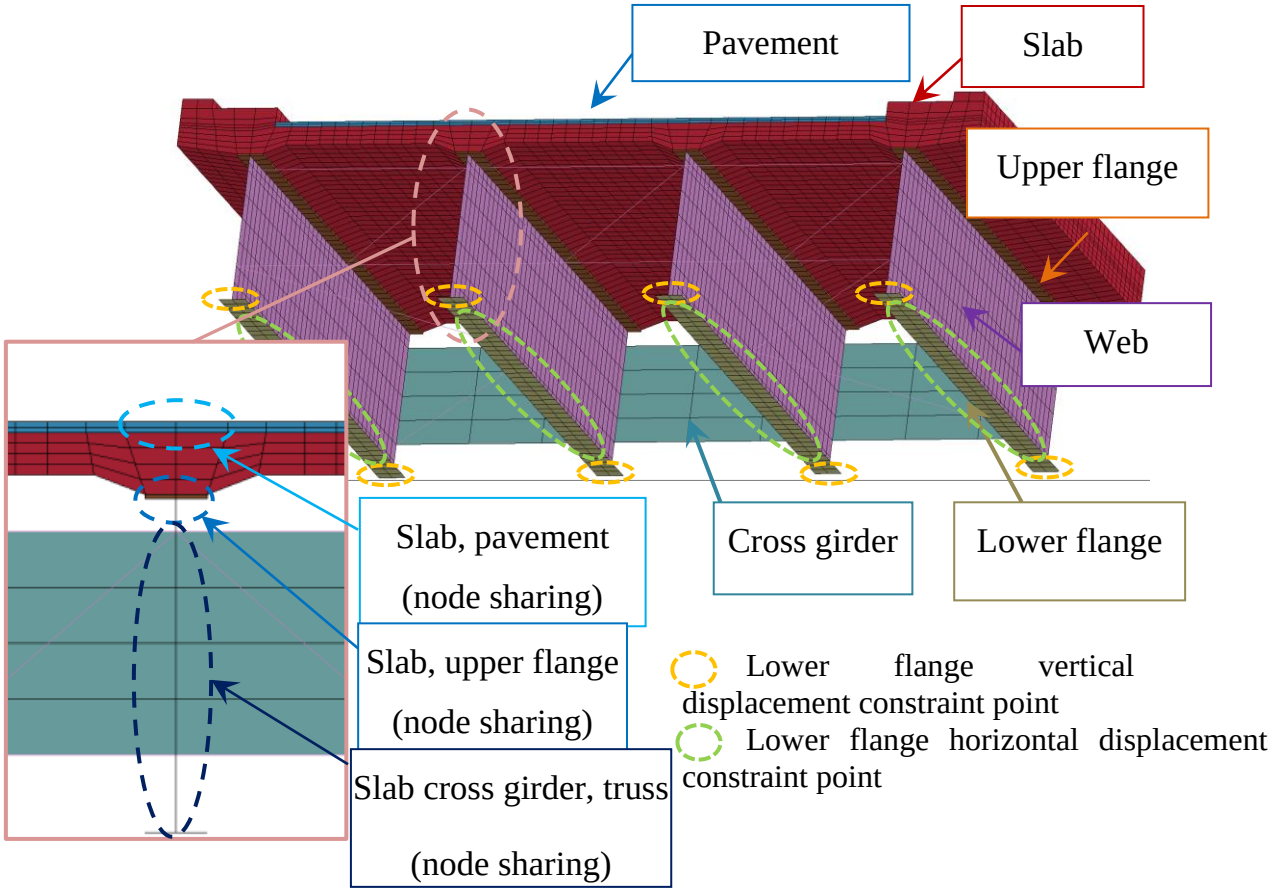


Figure 4.5: Solid partial model

Details of load application position and displacement measurement position will be described. The details of the load action position and the displacement measurement position on each model are shown in Figure 4.6 and Figure 4.7. The slab panels in each model are sectioned by yellow lines in each figure, and load application positions in each panel are set at the center of each. The displacement measurement positions in each model were set according to the distance between the displacement measurement positions in the actual test and the orientation of the accelerometer arrangement.

Setting of applied loads will be described. In the analysis in this study, since the calculation is performed with respect to the test at all loading positions, the time waveform of the load at each loading point is faithfully reproduced with the same operation time as that at the time of the experiment, but with regard to the load magnitude, the maximum value of 50 kN It was set by conversion. Moreover,

assuming that the impact force concentrates on the center of the loading board and is transmitted to the road surface, all the loading was carried out by the concentrated load.

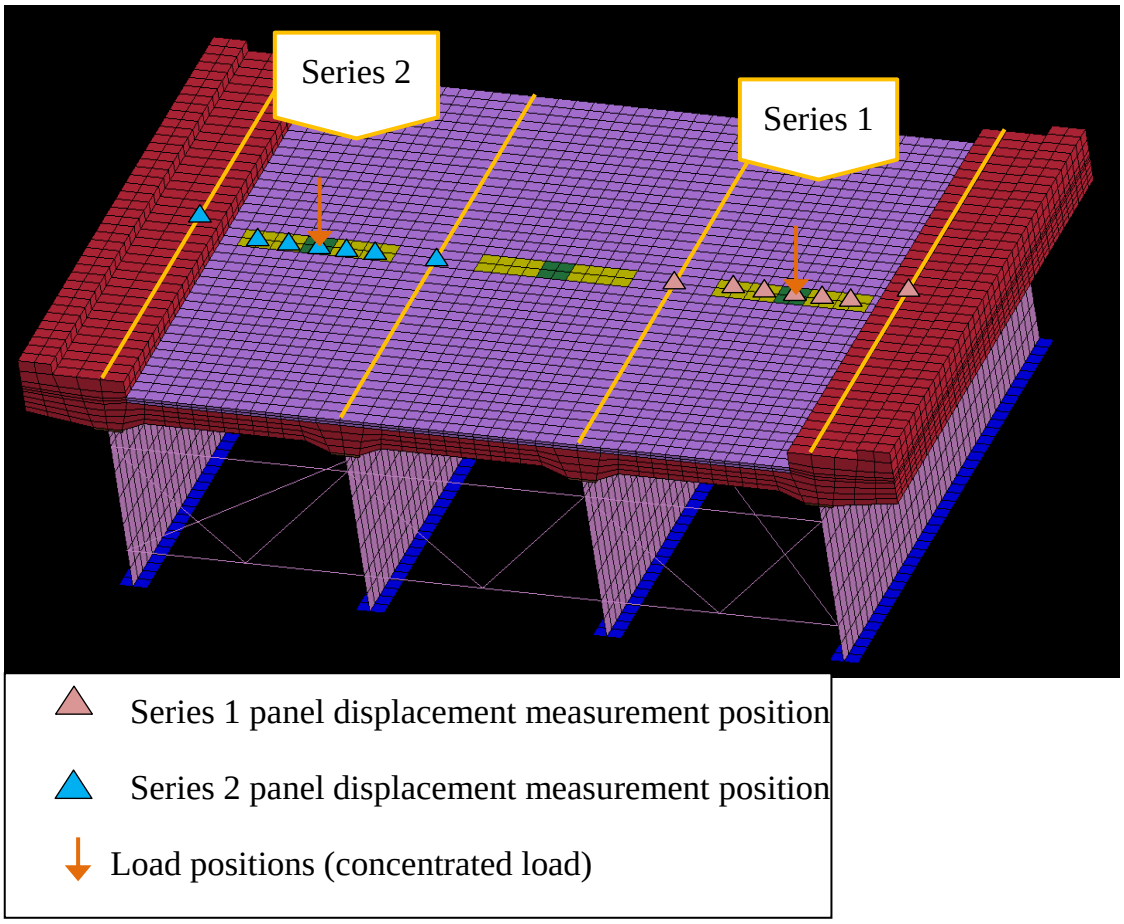


**Figure 4.6: Solid partial model**

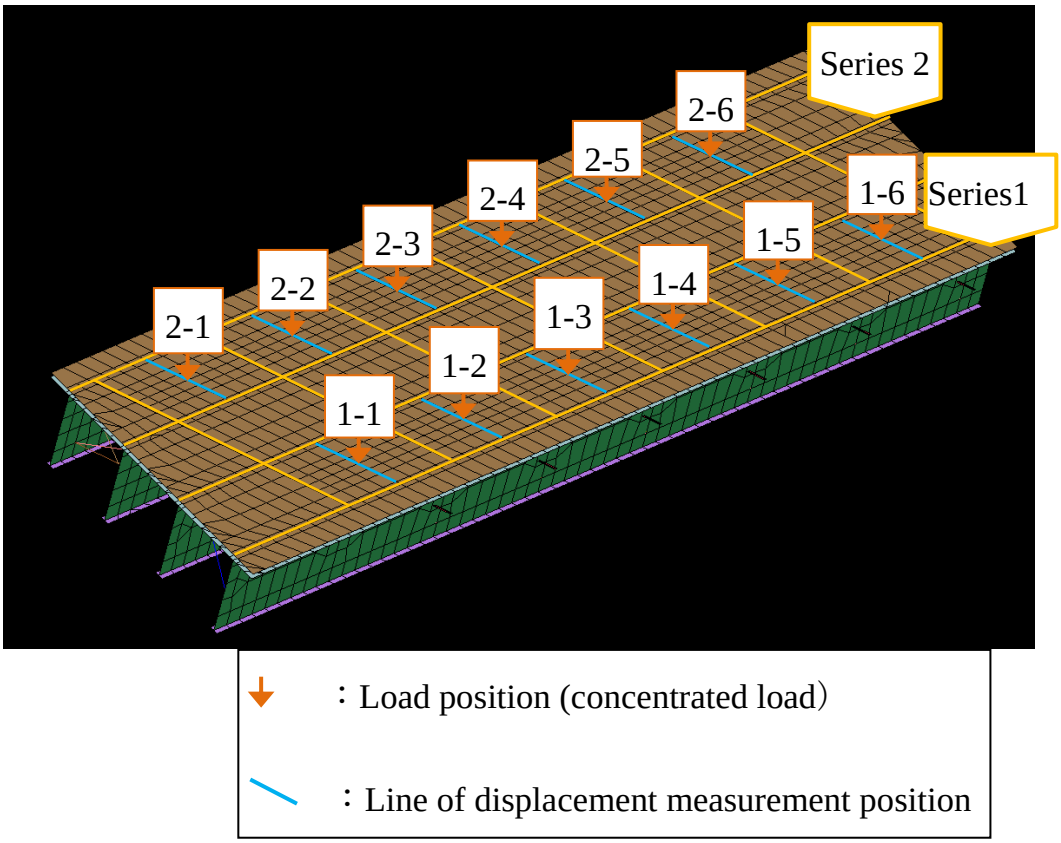


**Figure 4.7: Shell full bridge model**

### 4.1.3 Analysis results

Here we compare the distributions of pavement and slab displacement in the case of $E_c$ = 21.5 kN /mm$^2$and $E_p$ = 7 kN /mm$^2$ for both Hinoki Bridge shell model and Solid model.

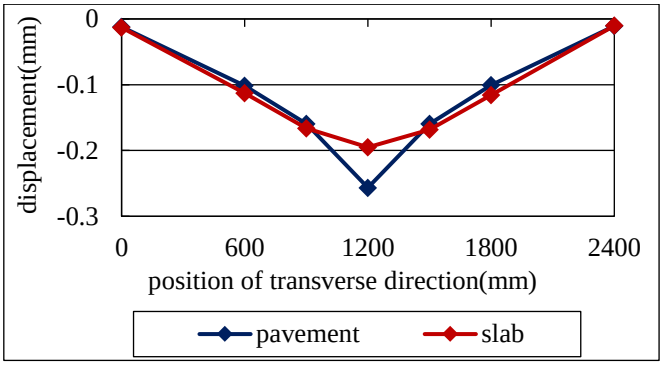


**Figure 4.8: Displacement distribution (solid model)**

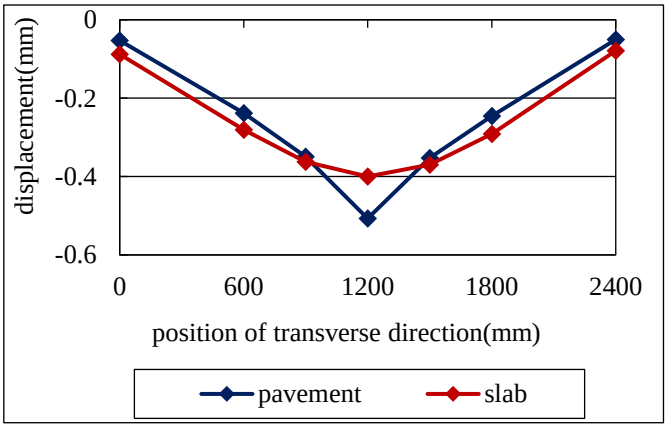


**Figure 4.9: Displacement distribution (shell model)**

Figures 4.8 and 4.9 compare the displacement distributions of the pavement upper surface and the deck lower surface of the shell model and the solid model, respectively. These displacement distributions show that when the displacement at the loading point shows the maximum value, and the displacement distribution on the upper surface of the pavement and the displacement distribution on the lower surface of the deck are necessarily those at the same time is not. In both models, the displacement distribution of the lower surface of the floor plate shows a distribution that is comparatively close to a parabol, whereas the displacement distribution of the

upper surface of the pave shows a distribution relatively similar to a parabola, except for the center, but the central displacement is sharp It is understood that it has the shape.

The displacement distribution on the pavement upper surface was consistent with the experimental result, suggesting that the abnormally large displacement measured in the actual test was caused by the influence of pavement deformation. In addition, it can be seen that the shell partial bridge model clearly has a different size, while the solid partial model shows almost the same value for the displacement of the spar position on the pavement upper surface and the floor lower surface. Owing to the difference in the way the bridge is reproduced by the model, and since the vertical displacement of the main girder is constrained, the displacement of the digit hardly occurs in the solid model, whereas in the shell model, the vertical displacement in the part is not constrained, it is thought that displacement occurs which is sufficient in size even in the main girder.

Comparison of pavement displacement due to temperature difference

The pavement has a different elastic coefficient depending on the temperature, the elastic modulus and loading of the deck are fixed (Ep = 21.5 kN/mm$^2$). Displacement on the pavement when showing the elastic modulus in the case of 5$^o$C ($E_p$= 10 kN/mm$^2$ ), 15 $^o$C (Ep = 7 kN/mm$^2$), 40 $^o$C (Ep = 0.938 kN/mm$^2$) And the displacement of the slab surface lower surface are obtained by analysis. This analysis was carried out with respect to Hinoki Bridge, using a shell model and a solid model. The analysis results are shown in Figures 4.10 and 4.11. From the results, it can be seen that the displacement of the pavement occurs largely only at 40 ° C, while the displacement of the pavement at 5 $^o$C and 15 $^o$C shows almost the same value. In addition, since the local temperature during the test in each target bridge was in the range of approximately 5 $^o$C to 15 $^o$C, it is considered that the influence of the temperature on the pavement elastic modulus at the time of the experiment hardly occurs.

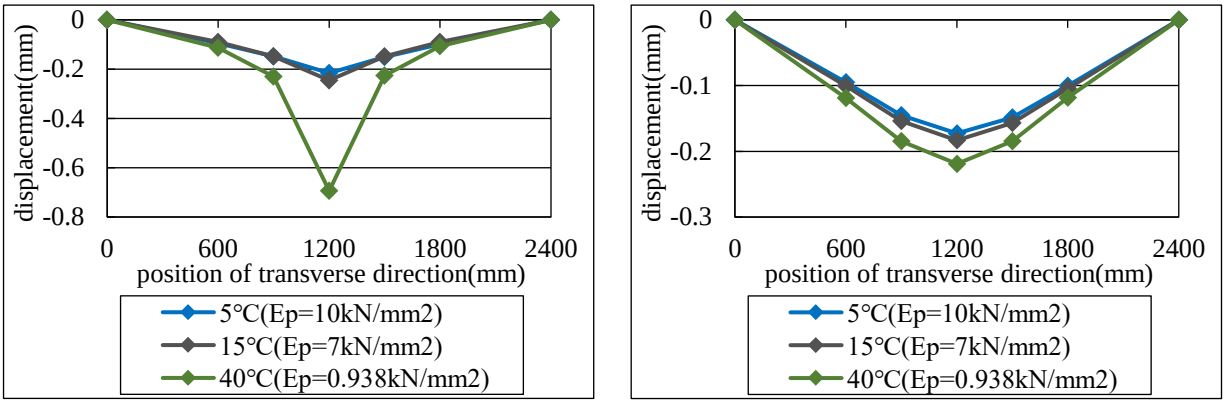


**Figure 4.10: Displacement distribution in solid model of pavement and slab**

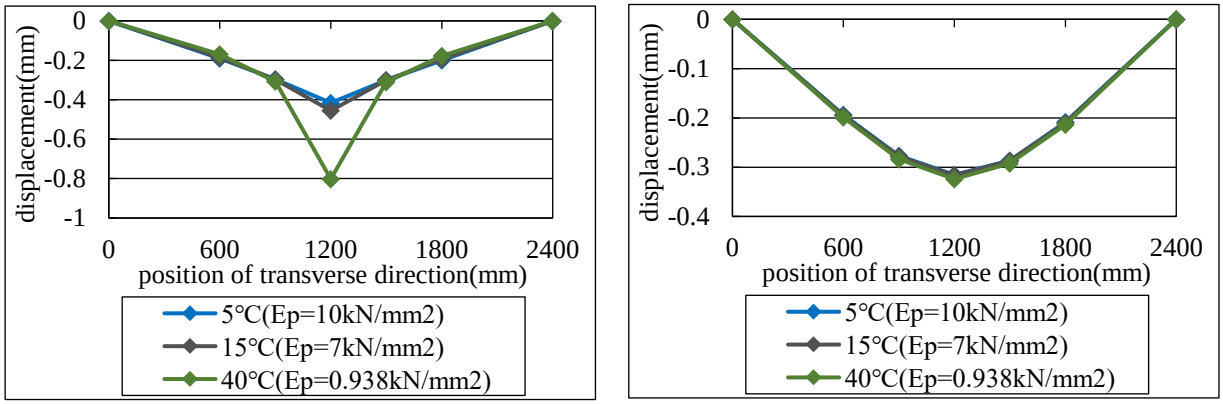


**Figure 4.11: Displacement distribution in shell model of pavement and slab**

The result of displacement at each loading position using shell model of Hinoki Bridge. At this time, the elastic modulus of the deck was unified with a fixed value, and the load was obtained by converting the actual loaded load to the loading point to 50 kN, and the shape of the time waveform was almost constant. These loading results are shown in Figure 4.12.

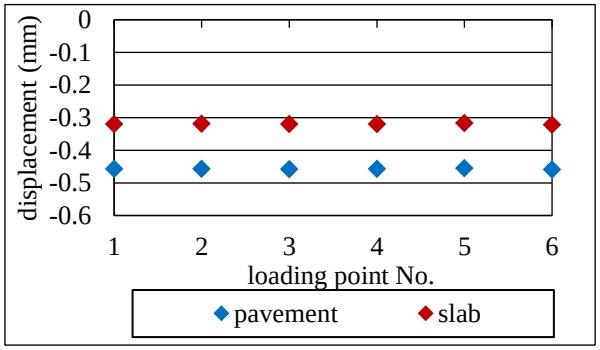


**Figure 4.12: Displacement value of all points in shell full bridge model**

From the results, if the elastic modulus of the deck is constant regardless of the end and center in the direction of the bridge axis at the bridge, the displacement of the deck will show an almost constant value when hitting the center of the panel. It is

considered that the influence of the position in the bridge axis direction on the displacement to the bridge slab is relatively small, and the elastic coefficient.

### 4.1.4 Comparison of displacement experimental and analysis results

For the displacement of each bridge on the lower surface of the deck, the analysis value is compared with the experiment value calculated by interpolation. Figures 4.13 and 4.14 show the comparison of bridge and each series.

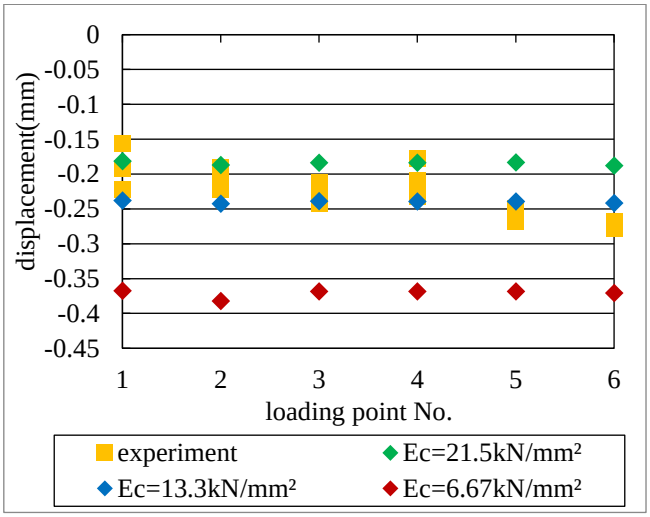


**Figure 4.13: Comparison of experiment value and analysis value series 1**

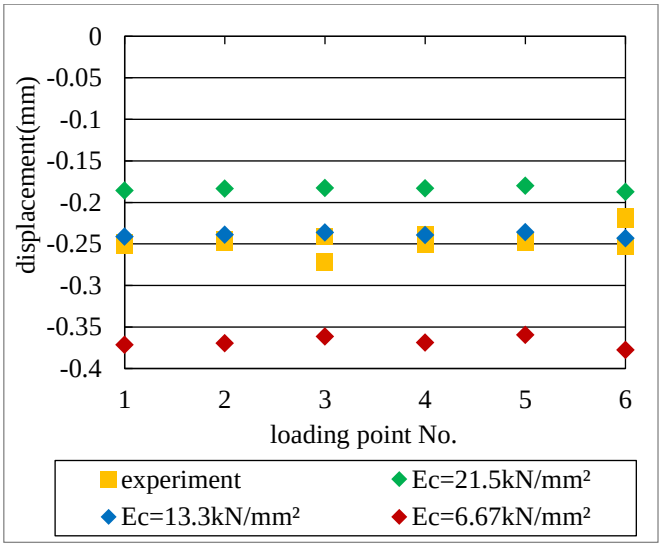


**Figure 4.14: Comparison of experiment value and analysis value series 2**

These results are compared with the actual deterioration situation.

In Hinoki Bridge, leakage occurred in any panel from the actual deterioration situation, in particular, the wetting range of the spar end portion is larger than that of the position in the middle of the span, white precipitate also exudes, which clearly indicates that relatively severe deterioration occurs in the actual slab. From this and the comparison of the above analysis value and experimental value, it was possible to infer the presence or absence of deterioration, but we can see that the estimation of the degree of deterioration.

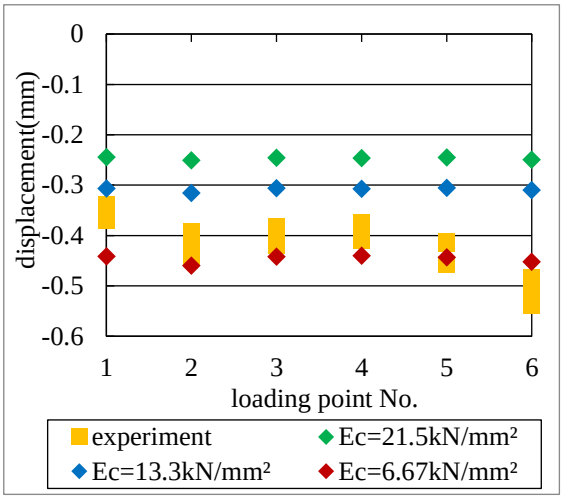


**Figure 4.15: Comparison of experiment and analysis displacement of upper pavement series 1**

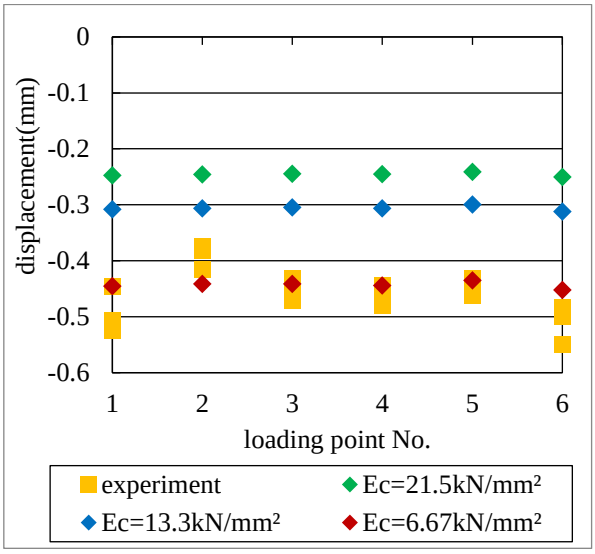


**Figure 4.16: Comparison of experiment and analysis displacement of upper pavement series 2**

For the displacement of each bridge on the pavement upper surface, compare the analysis value with the experimental value. Comparison of each bridge and each row is shown in Figure 4.15 and 4.16.

In Hinoki Bridge, leakage occurred in any measurement panel in the actual slab, clearly indicating that relatively severe degradation occurred. From this and the comparison of the above analysis value and experiment value, it is considered that the degree of deterioration can be inferred. Moreover, from the comparison of the analysis value and the experimental value, the panel (1-6, 2-1, 2-6) in the vicinity of a part of the girder end has more severe deterioration phenomenon than the other same panel. However, from the appearance observation, it was impossible to determine whether there was a clear difference between the degree of deterioration of the panels and the degree of deterioration of other panels. However, the girder end panel located immediately adjacent to the spar side as viewed from the panel clearly has more severe deterioration as compared with other panels, such as leaking water covering the entire surface thereof and exudation of white precipitates occurred. There is a possibility that the influence of the deterioration may be exerted on the panel near the corresponding girder end, which seems to have appeared in the magnitude of the displacement experiment value.

## 4.2 Yatsuo Bridge

### 4.2.1 Analysis method

For the bridge considered in this study, a finite element method analysis (LS-DYNA) was conducted to reproduce the displacement distribution when the impact loads with the same operation time as those in the experiment were loaded onto each panel [10]. A shell element is used for the steel girder, the RC deck slab and pavement were simulated as solid elements, and a beam element was used for other parts, such as the cross bar. The thickness of the RC floor slab is 200 mm, and the pavement thickness is 50 mm. Regarding the boundary condition, only the displacement of the lower flange at both ends of the span was constrained, and the rotations of the lower flange in the x- and y-directions were restrained. In addition, to make the positional

join between the RC floor slab and the pavement the same as the actual bridge, these members were brought into contact.

### 4.2.2 Analysis model

The material property values are shown in Table 4.3. The material properties of all members were linear elastic bodies. According to past studies [1], the elastic modulus of the concrete is determined through a comparison with the experimental value to evaluate the degree of deterioration of the bridge deck, and the limit condition of the Young's modulus ratio of concrete to steel of n = 15 was used as the reference for the usability of the bridge, and n = 30 was applied as the ultimate limit state.

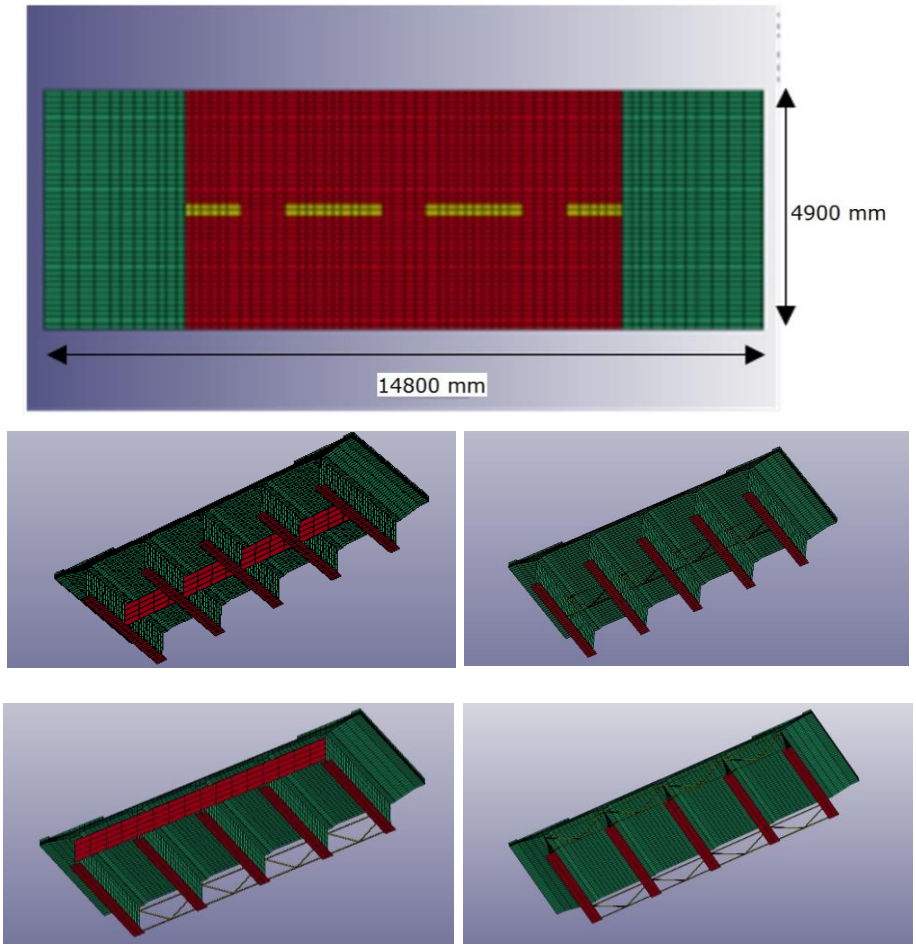


**Figure 4.17: Yatsuo analysis model**

The ratio at a state close to the ultimate limit was used. Regarding the modulus of elasticity of the pavement, the formula given in [11] was used. As is known from

practical research [1], there is no practical problem in an evaluation when changing the Young's modulus of the concrete, and an internal rebar has not been modelled.

Because concrete is an effective elastic region in all cross sections in the analytical model, it is considered that the influence of the internal reinforced steel is almost zero, and reinforced steel was not considered in this analysis model. A load waveform, which was corrected such that the waveform of the impact load measured experimentally at each loading point became 50 kN, was used for the analysis. The load waveform was applied as a concentrated load at the center of each panel; in addition, and the displacement of the pavement surface at the point of the accelerometer position actually measured at the time of the experiment, and the displacement of the lower surface of the deck, were calculated in the generated analysis model.

**Table 4.3: Material properties**

| Material | Young's modulus ($kN/mm^2$) | Poisson's ratio |
|---|---|---|
| Concrete | 13.3(n = 15) | 0.2 |
| | 6.67(n = 30) | |
| Steel | 200 | 0.3 |
| Asphalt | 7 (for 15 °C) | 0.35 |

### 4.2.3 Analysis results

Displacement based on calculations is influenced from the sinking of a steel girder. Therefore, the relative displacement distribution obtained by subtracting the vertical displacement of the girder such that the displacement at the steel girder position is zero is defined as the displacement when the elastic modulus of the pavement is E = 7 kN/mm2 (15 °C.). The first impact of points 2–5 is shown as an example (Figure 4.18). In this figure, A is the displacement distribution when the loading point displacement of the pavement surface reaches the maximum value, B is the displacement distribution measured from the lower surface of the deck at the same

time as the distribution of A, and C is the maximum displacement of the loading position of the lower surface of the deck.

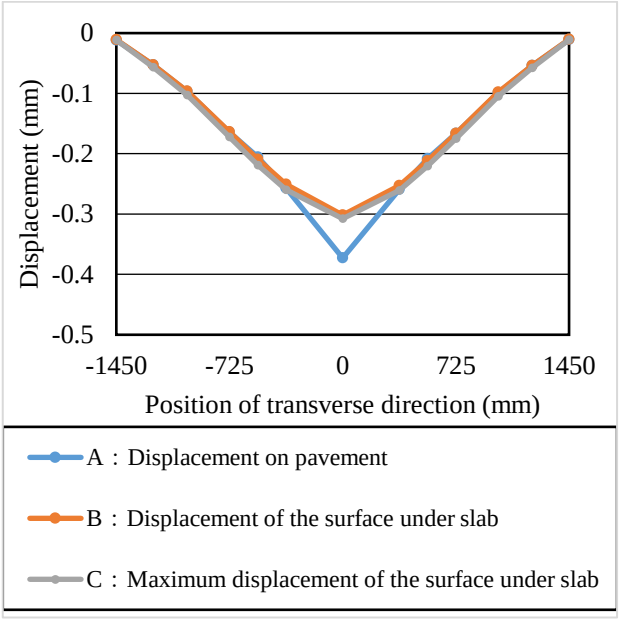


**Figure 4.18: Example of analysis results for points 2–5**

Furthermore, the time history of the loading point displacement, including the displacement of the steel girders A, B, and C, is shown in Figure 4.19. Comparing A and B from Figure 3.27, B is a smooth parabola, whereas A shows that only the displacement of the load point is a large value.

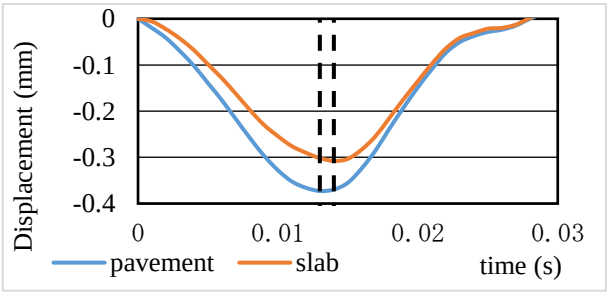


**Figure 4.19: Displacement on pavement surface and lower surface of slab**

Moreover, the experimental results of the displacement measured on the pavement are similar to the distribution shape of A. Based on this fact, as a result of comparing A and B, and the experimental values, the displacement distribution of B was not measured during the experiment; however, the displacements other than the loading point generally agree. From this, it can be stated that only the displacement of the

loading point has an influence on the pavement settlement. In addition, when comparing B and C, it is understood that the values are relatively close to each other. In other words, it can be stated that the displacement of the floor plate when the loading point from the pavement is at the maximum displacement nearly coincides with the distribution when the floor plate of the loading point reaches the maximum displacement. This tendency was the same even when the pavement showed another elastic modulus.

### 4.2.4 Comparison of displacement experimental and analysis results

It is clear from the analysis that the displacement distribution nearly coincides with the analysis distribution. In other words, if the displacement of the pavement surface at the loading point is removed, it is assumed that the degree of degradation of the deck can be compared with the analysis from the maximum displacement at the loading point of the deck. In view of this, we used the interpolation of the loading point displacement of the deck using Newton's interpolation for the experimental values converted into the maximum load of 50 kN, along with the displacement of the deck obtained from the analysis using the elastic coefficient Ec = 13.3 kN / $mm^2$ (elastic modulus ratio n = 15) and the state near the ultimate limit of the elastic modulus Ec = 6.67 kN / $mm^2$ (elastic modulus ratio n = 30).

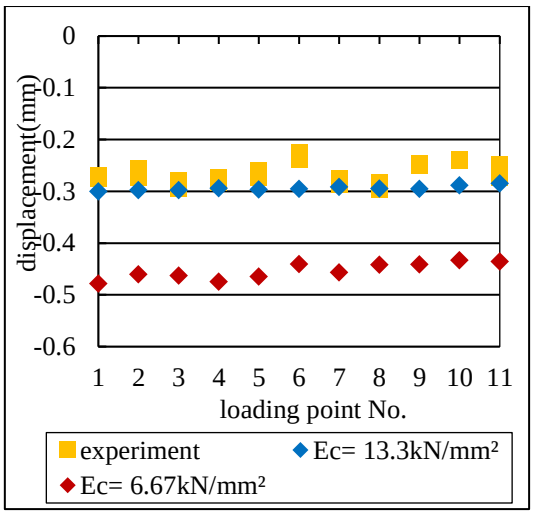


**Figure 4.20: Comparison of series 2 results**

As a result, in series 2 (Figure 4.20), the interpolated value of the experimental displacement was close to the usage limit state obtained from the analysis of the slab.

In series 3 (Figure 4.21), it was found that the interpolation value of the experimental displacement exceeded the displacement of the usage limit state obtained from the analysis of the slab, but did not exceed the ultimate limit state. In addition, at a point where deterioration, such as a leakage, occurred, a large displacement was obtained, as compared to the other loading point.

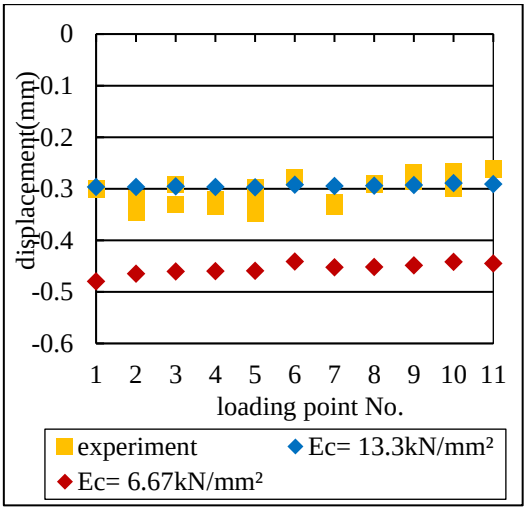


**Figure 4.21: Comparison of series 3 results**

Based on this fact, it is necessary to continue the observation of damage to the bridge because the displacements in the calculation under limited conditions are shown from series 2 and 3. Specifically, when the damage progression is confirmed during the next bridge inspection, it is assumed that the same loading test implementation will be effective in terms of determining the amount of damage.

### 4.3 Summary

It was suggested that the state degraded to some extent from the healthy state can be estimated for the degradation degree from the lower surface displacement of the deck. However, in some panels, although the actual deterioration was found, the degree of deterioration was small, which was the result of estimation. This is considered as one of the reasons why the value used for the experimental value is an interpolated value calculated from displacement on the pavement and not necessarily coincident with the actual slab displacement.

For the estimation of deterioration degree from the pavement top surface displacement, it was inferred that severe deterioration occurred from the comparison between the analysis value and the experiment value at the place where severe deterioration was observed in observation from the lower surface of the deck. In addition, it was inferred that degradation phenomenon of cracking degree or severe degradation phenomenon occurred in the part where only damage such as cracks was found. In the analysis, when the displacement of the loading point reaches the maximum values, the displacements of the other points are clearly in agreement when comparing the pavement and deck slab.

From the above, it was shown that the deterioration degree of the deck can be estimated from the displacement of the pavement upper surface. When the damage progression is confirmed during the next bridge inspection, it is considered that an implementation of a similar load test at this time will be effective from the viewpoint of determining the degree of damage.

# Chapter 5: Reinforcement effect by carbon fiber for Fatigue-damaged concrete slabs

## 5.1 Overview

The number of aging bridges increases certainly in Japan, maintenance and management of them become an unavoidable social issue. Therefore, the planning of effective countermeasures for damaged bridge is one of urgent important issues. In the present situation, the bridge inspection legislated in 2014 has been proceeding in Japan [1,2]. The grasp of damage degree and implementation of repair countermeasures corresponding the results of bridge damage have been executed mainly on the national highway.

However, the most of domestic bridges under local municipal management actually are not efficiently taken care due to lack of engineers and financial shortage. It is considered necessary to give a reasonable judgment method to select two ways, which specifically is the way ensuring the required performance by repair and reinforcement and the way prolonging the life until the next countermeasure [3,4].

Therefore, in this research, in order to provide the reinforcement method to improve load bearing performance and the method that can be expected to prolong life even if improvement of load bearing performance cannot be anticipated, experimental research had been done.

## 5.2 Experiment outline

### 5.2.1 Specimen of concrete slab

The specimens were full size, specimen A was conformed to the specification of road bridge in 1964 (Showa 39 era). The amount of reinforcing bar and thickness of the deck slab were specified as B specimen which is compliant with 1972 (Showa 47 era) specification road bridge. Two types of test specimens were produced Figure 5.1 and Figure 5.2 shows respectively specimen of concrete slab A and specimen of concrete slab B.

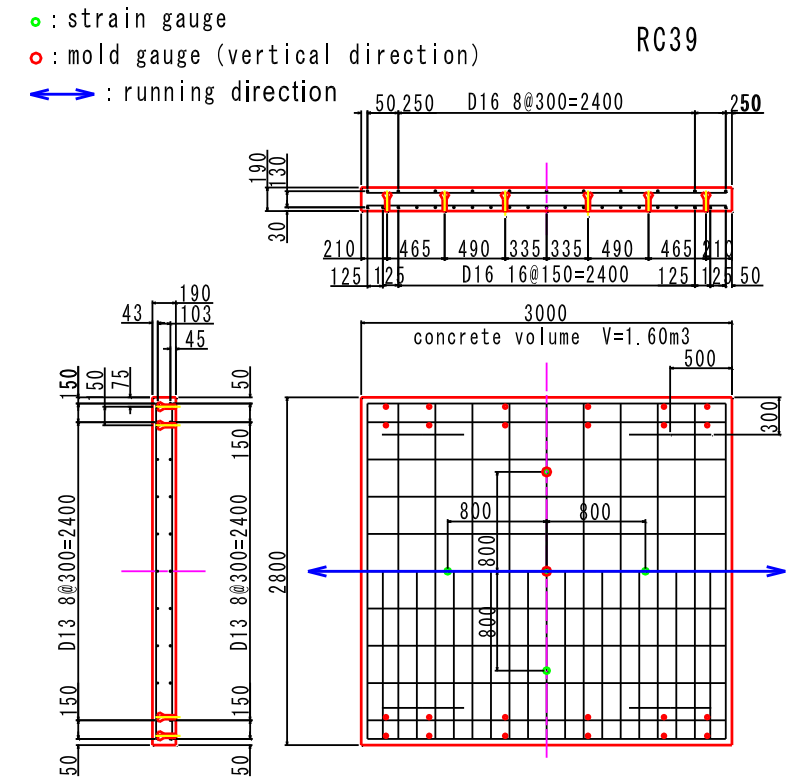


**Figure 5.1 Specimen A**

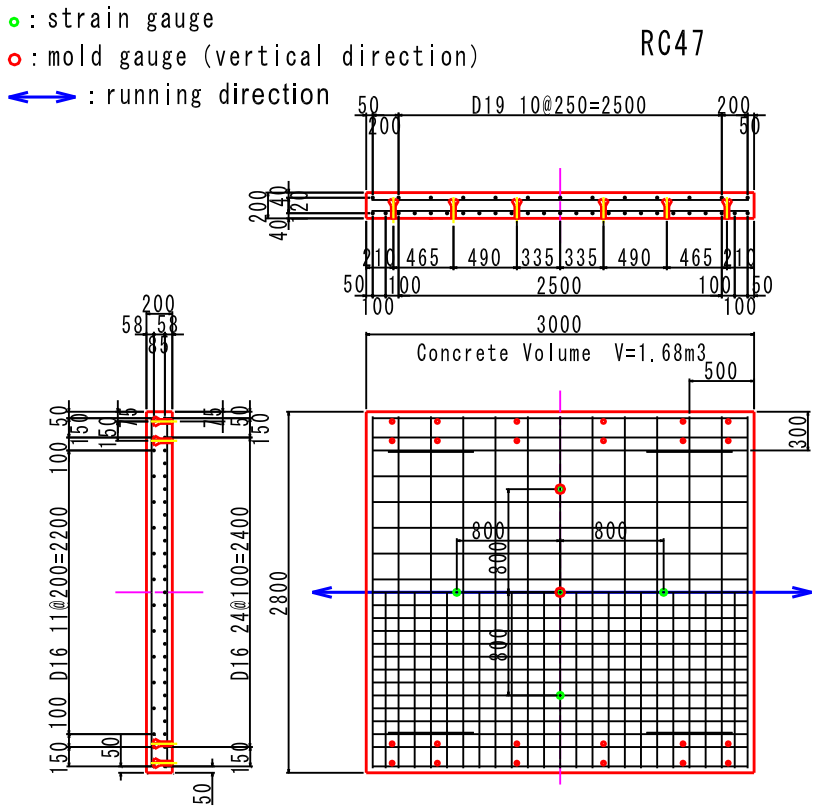


**Figure 5.2 Specimen B**

**Table 5.1 Thickness of concrete slab and amount of steel reinforcement**

| Name of specimen classification | Thickness of slab (mm) | Arrangement of steel reinforcement |
|---|---|---|
| A | 190 | Bridge axis direction upper side D13x11, lower side D13x11<br>Bridge axis orthogonal direction upper side D16x11, lower side D16x21 |
| B | 200 | Bridge axis direction upper side D16x16, lower side D16x27<br>Bridge axis orthogonal direction upper side D19x13, lower side D19x25 |

The amount of reinforcing bar and the thickness of the deck plate are shown in Table 5.1, and the concrete properties are shown in Table 5.2. In this experiment, it is thought Young's modulus of specimen B is small because of water- cement ratio. This is similar to the Young's modulus decrease sometimes observed damaged concrete by the Alkali silica reaction (ASR) etc.

**Table 5.2 Characteristics of concrete**

| Name of specimen | Compression strength $f'_{ck}$ ($N/mm^2$) | Young's modulus $E_c$ ($kN/mm^2$) | Poisson's ratio |
|---|---|---|---|
| A | 40.4 | 33.5 | 0.146 |
| B | 21.3 | 7.99 | 0.150 |

The reinforcement was made for each specimen by inserting a rod of carbon fibers grooved on the lower surface of the deck slab and impregnated with epoxy resin. Table 5.3 shows the material characteristics of used carbon fiber. Strength of used epoxy resin is shown in Table 5. 4.

**Table 5.3 Material characteristics of used CFRP strand**

| Material for reinforcement | Carbon Fiber Reinforced Plastics |
|---|---|
| Weight per unit length (g/m) | 254 |
| Sectional area ($mm^2$) | 44 |
| Young's modulus ($kN/mm^2$) | 231 |
| Tensile strength ($N/mm^2$) | 4,639 |
| Rigidity (kN) | 10,164 |

**Table 5.4 Strength of used epoxy resin**

| Item | Value | Test Method |
|---|---|---|
| Tensile strength ($N/mm^2$) | 52 | JIS-K7161 |
| Bending strength ($N/mm^2$) | 63 | JIS-K7171 |
| Tensile shear strength ($N/mm^2$) | 20 | JIS-K6850 |

By inserting it into the groove cutting (15mm*15mm*2400mm), deterioration progression after reinforcement can be confirmed, and even when water leakage due to a defect of the waterproof layer occurs, it does not stay inside the slab. One strand consisted from 48 bundles of carbon fibers is roughly equivalent to two layers of a general 300 g basis weight and regular length of the strand sheet is 50 m. Therefore, it is possible to construct without a joint until the length 50 m. Additional work does not occur at a construction site of a real bridge which takes time and effort concerning

a joint problem. After an experiment on simple beam with reinforcement of carbon fiber with the quantity 48 and 72 respectively, we decided to use 48 bundles of carbon fiber for this experiment due to the effectiveness of strength and cost.

Reinforcing materials were installed in only one direction of the bridge axis in the A specimen with 15 rods of carbon fiber. While the B specimen was set in two directions of the bridge axis perpendicular and the bridge axis. This is because fatigue deterioration has developed greatly in many cases due to the low loading performance of the 1964 edition road bridge specification book (Showa era 39), although replacement is desired as a drastic response. The direction of reinforcement was set as the bridge axis direction because it is known that the S39 roadbed slab is subjected to punching shear fracture after the formation of beams from plate due to fatigue deterioration in a past study. If the formation of beams from a plate can be prevented, it is expected that this prevention method will contribute to extending the life by reinforcing in the bridge axis direction.

### 5.2.2 Wheel load running test

The purpose of this research is to confirm the reinforcement effect after reproducing the degradation process of the actual bridge deck, a crank type testing machine from preliminary loading by a testing machine equipped with rubber tires (Figure 5.3).

**Figure 5.3 Wheel load running test machine**

The slab was fixed to the supporting girder with bolts in this test. After reinforcement with CFRP rods, the loading carried out by crank type running test machine (Figure 5.4), in this test, the slab was simply supported with round bar.

**Figure 5.4 Crank type running test machine**

Table 5.5 shows the loading load and the shape of the active area of load. The table also shows the number of runs for each type of loading, but in this loading, it has been running 100,000 times by checking the deflection increasing tendency at 160 kN, and that number is also included.

**Table 5.5 Load and active area**

| Name of specimen | Load classification (Number of load running: thousand times) | Loading force (kN) | Active area of load Bridge axis direction×orthogonal direction (mm) |
|---|---|---|---|
| A | Preliminary loading (135.0) | 160 | 350×450 |
| | Loading (436.2) | 160 to190 | 120×300 |
| B | Preliminary loading (215.2) | 160 | 350×450 |
| | Loading (360.9) | 160 to 230 | 120×300 |

### 5.3 Experiment results

#### 5.3.1 A specimen

A specimen was reinforced by CFRP rods in one direction (Figure 5.5)

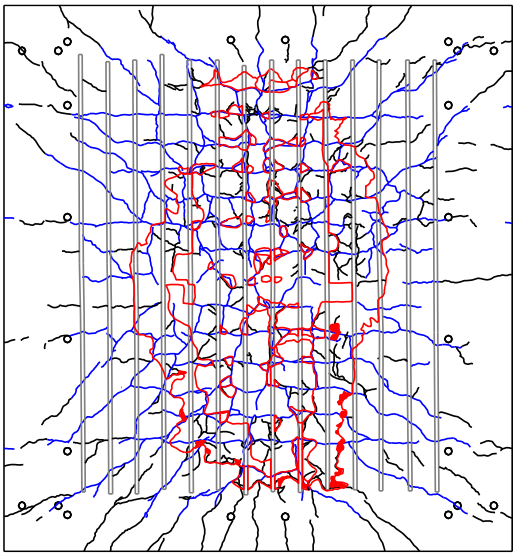

— Preloading cracks — Running test loading cracks □ Peeling/ Spalling

**Figure 5. 5 Specimen A reinforced direction and cracks**

The changes over time in the deflection of the A specimen of the preliminary loading and the final load after reinforcement are respectively shown in Figure 5.6 (a) and (b).

"Loading" shown in Figure 5.6(a) of preliminary loading is the measured value of the deflection statically loaded at each fixed number of runs, "Unloading" is the value with no load, "Loading-Unloading" is corresponding to the elastic component. In addition, three results of deflection by elastic calculation are shown. They are the calculation value using the actual Young's modulus $E$= 33.5 kN/mm$^2$, the calculation value corresponding to Young's modulus ratio of steel and concrete n= 15 and the calculation value to the ratio n= 30. It is generally known that n= 15 is approximately same as the condition neglecting tension area of concrete and n= 30 is nearly to the ultimate state. For the support condition in calculation, it was assumed that the direction of the bridge axis was fixed on the supporting beam fixed by bolts and the direction orthogonal to the bridge axis was simply supported on the support beam. From this figure, it can be estimated that state of the specimen is close to the ultimate

state, because the deflection at "Loading - Unloading" exceeds to the deflection where the calculated assumed n= 30.

The load in shown in Figure 5.6 (b) is equal to the load of the preliminary loading 160 kN up to 1.35E+05 times. Deflection " Loading - Unloading" is same as that in the preliminary loading, although the shape of the loading surface is different.

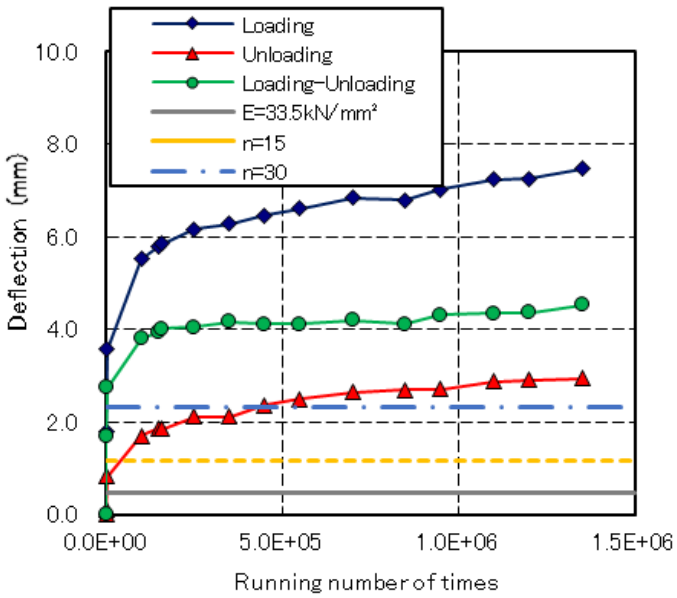


(a) Preliminary loading

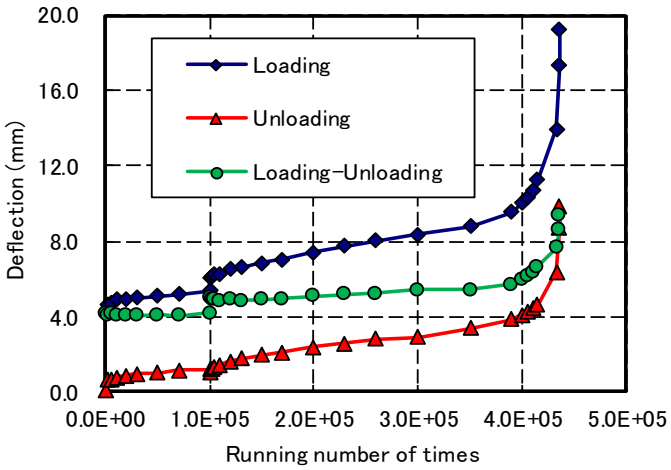


b) Loading after reinforcement

**Figure 5.6 Change of deflection of center point with time (Specimen A)**

It can be seen that reinforcing effect due to decrease of deflection is not obtained, because reinforcements are only in the direction of the bridge axis. After confirmation that the increase of deflection is almost stopped at 100,000 times for the load of 160

kN, the running experiment was continued under the increased load 190 kN. The experiment was completed at the number of runs of 436.2 thousand times. Steps were observed in wide area at the lower face of specimen. It can be thought that the specimen finally reached to the pushing shear failure by those occurred steps.

**Figure 5.7 The fixing end of carbon fiber after experiment**

However, just before the shear fracture, concrete fracture occurred at the fixing end of the fiber as shown in Figure 5.7, and it was confirmed that as a trigger by this fracture the fracture was transferred to the interior of the specimen and reached to general punching shear fracture. Its process is different from general punching

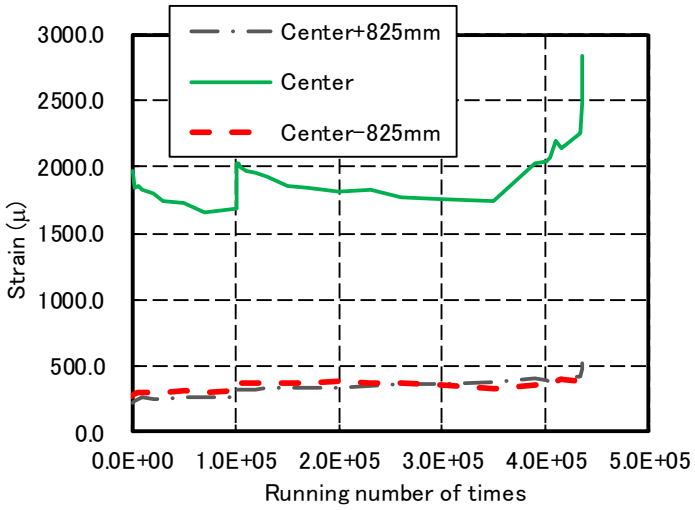


**Figure 5.8 Change of strain of carbon fiber reinforcement with time**

The change with time of the strain of the carbon fiber is shown in the Figure 5.8. The strain at the center is 1700 to 1800 μ, whereas the strain generation amount is about 400 μ at the position 825 mm away from the center, which is roughly quarter of the center. It became clear that the carbon fiber rod immediately under the wheel

load is effective for reinforcement. It can be estimated that there is considerable life prolonging effect of concrete slab by this reinforcement, even if the reinforcement is performed only under the wheel load and in the vicinity thereof (for example, the range of 45 ° below the cross section from the loading end).

Figure 5.5 also shows the cracks after entire test of specimen A. In this figure the crack with blue deformed after preloading test, after all the test some part of the slabs had been peeled out or spalled.

### 5.3.2 B Specimen

The direction of CFRP rods in specimen B was showed in (Figure 5.9) with two direction.

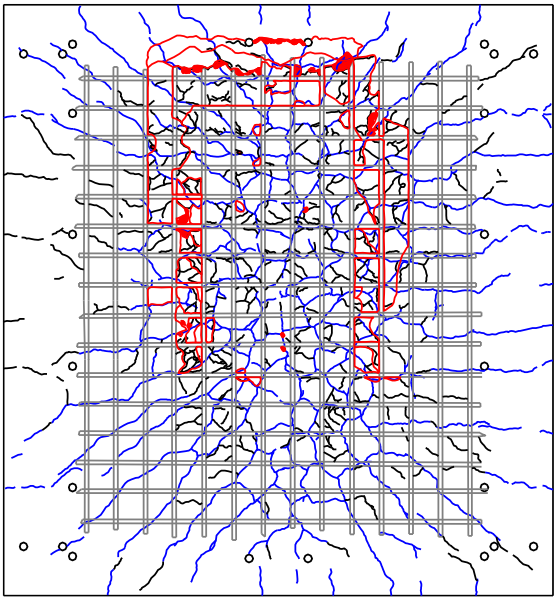

— Preloading cracks — Running test loading cracks □ Peeling/ Spalling

**Figure 5.9 Specimen B reinforced direction and cracks**

The changes over time in the deflection of the B specimen of the preliminary loading and the final load after reinforcement are respectively shown in Figure 5.10 (a) and (b). Figure 5.10 (a) also shows the deflection calculated by the Young's modulus by the compression test on the specimen at the time of concrete casting by the same method as the A specimen. Young's modulus of this specimen is lower than that of specimen A, therefore, the deflection of "Loading - Unloading" increased to 3.22 mm, which is approximately twice of the calculated value 1.67 mm at the end of preliminary loading. It means that fatigue deterioration has developed exceeding the

serviceability limit. Since the specimen is reinforced in two directions, the deflection at the time of loading - unloading was reduced to 2.20 mm at the start of the final loading after reinforcement. Therefore, it was confirmed that the rigidity was improved by reinforcement.

Figure 5.10 (b) shows the change of deflection with time after reinforcement. The deflection sharply increased at 360.8 thousand times and the experiment was completed. Steps were observed in deflection of the lower surface. It is considered that the punching shear fracture caused these steps.

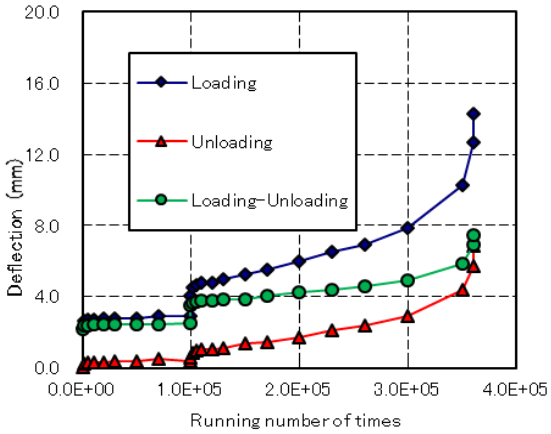


(a) Preliminary loading

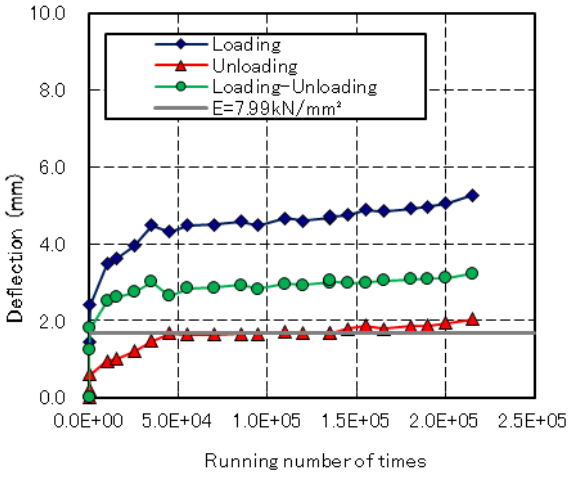


(b) Loading after reinforcement

**Figure 5.10 Change of deflection of center point with time (Specimen B)**

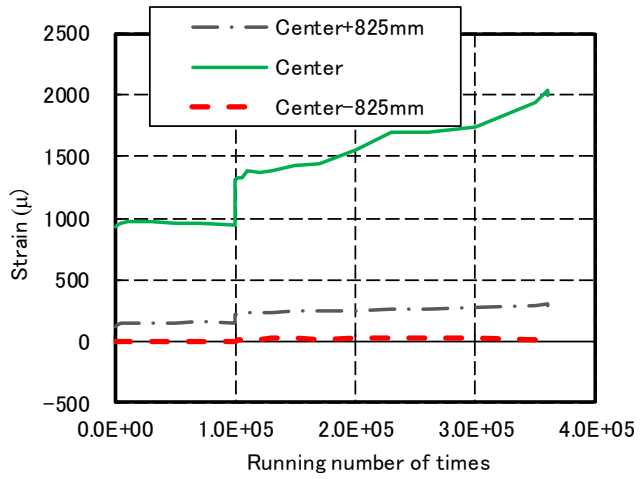


a) Strain of bridge axis direction in the orthogonal

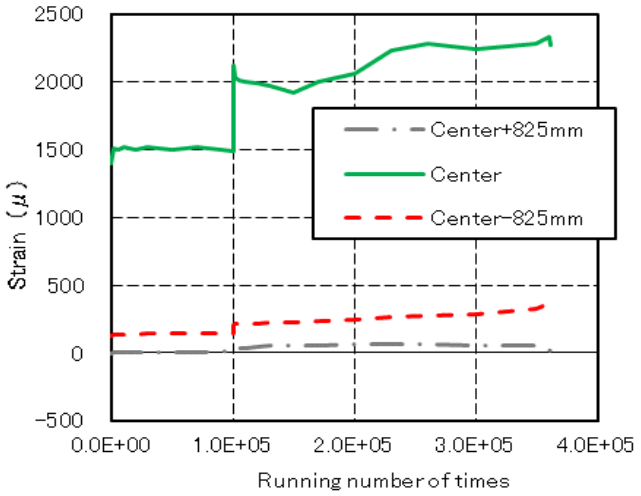


(b) Strain of bridge axis orthogonal direction in the center cross section

**Figure 5.11 Change of strain of carbon reinforcement with time**

The changes of strain of the carbon fiber are shown in Figure 5.11 (a) and (b). Figure 5.11(a) shows strain in the direction perpendicular to the bridge axis, the measured value at the center exceeds 2000 μ in the latter half of the experiment. Both strains at the position 825 mm away from the center are small under 350 μ. On the other hand, in the Figure 5.11 (b) showing strain in the bridge axis direction, the strain at the center as a somewhat is lower level of 1500 to 2000 μ. Strains at the position 825 mm away from the center are small under 350 μ.

In Figure 5.9 shows the cracks of B specimen after entire test. After preloading, the running test makes the cracks developed more and some part of the slab seemed to be peeled and separated.

### 5.4 Evaluation of fatigue durabilities

It is considered that the reinforcement effect can be grasped using the SN curve obtained from the results based on the previous road experiments by the same wheel load- running machine used in the past. The equivalence number of runs by the same load of 160 kN is calculated by following equation [5].

$$\mathrm{Log}(P/P_{sx}) = -0.09121\mathrm{Log}N_{eq} + \mathrm{Log}1.52 \qquad (1)$$

Here, $P$ is wheel load (kN), $P_{sx}$ is punching shear strength and $N_{eq}$ is equivalent load running number. The calculation formula is based on $P_{sx}$ in consideration of the formation of beams from a concrete slab by Matsui. The reinforcing layer with carbon fiber are not considered in this equation. Calculation results are as shown in Table 5.6, and a reinforcement effect of 10.14 times against that of non-reinforcement is obtained. Therefore, it can be expected that sufficient reinforcing effect can be expected, and it is considered to have a life prolonging effect.

**Table 5.6: Calculation results concerning Fatigue Durability**

| **Items** | **S39-2 (No reinforcement)** | | **S39-2 （A specimen）** | | **S47-2 (No reinforcement)** | | **S47-2 (B specimen)** | |
|---|---|---|---|---|---|---|---|---|
| Compression strength $f'_c$ （N/mm$^2$） | 49.6 | | | | 25.2 | | | |
| Young's modulus $E_c$ （kN/mm$^2$） | 34.3 | | | | 8.0 | | | |
| $P_{sx}$ （kN） | 326.9 | | | | 381.3 | | | |
| Loading program | $P_i$ | $\Delta N_i$ | $P_i$ | $\Delta N_i$ | $P_i$ | $\Delta N_i$ | $P_i$ | $\Delta N_i$ |
| | 160 | | 160 | 100,000 | 160 | | 160 | 100,000 |
| | | | 190 | 315,000 | | | 230 | 250,000 |
| $P/P_{sx}$ | 0.49 | | 0.49 | | 0.42 | | 0.42 | |
| Equivalent number $N_{eq}$ （$P$=160kN） | 214,187 | | 2,171,548 | | 15,440,759 | | 13,445,108 | |
| Reinforcement effect | 1.00 | | 10.14 | | 1.00 | | 0.87 | |

In the B specimen, although not evaluated by the SN curve, fatigue durability is thought to be improved in view of the fact that the Young's modulus is small concrete and fatigue deterioration has progressed even in preliminary loading. However, it is thought that further detailed investigation is necessary for the quantitative reinforcement effect. The implementation to conduct additional experiments is scheduled

### 5.5 Summary

In this research, as a countermeasure for deteriorated bridge concrete slabs, we propose a method of inserting rods of carbon fibers impregnated with resin in grooves on the lower surface of the concrete slab and confirming the reinforcing effect by the wheel load running experiment. The obtained results are shown below.

(1) The specification of road bridge in 1964 (Showa 39 era) ‘s specimen A was near fatigue deterioration state in preliminary loading. However, the life of specimen A was postponed by carbon fiber reinforcement in only the direction of the bridge axis. Reinforcing effect of 10.14 times as an equivalent to the number of running times was obtained.

(2) It has become clear that the reinforcing effect can be obtained only by reinforcement in the range where the load acts, because the strain of the carbon fiber of the A specimen is large just under the wheel load and strain in the vicinity of the support is quarter.

(3) In the B specimen with a small Young's modulus, the effect of reducing deflection by carbon fiber reinforcement in two directions was confirmed and it is considered that an improvement in fatigue durability could be expected. However, in the confirmation of the quantitative effect, further examination is required.

In the future, we are going to conduct a confirmation experiments on fatigue durability by wheel load running experiment for deteriorated bridge slab by ASR, and we are planning to examine whether carbon fiber reinforcement shown in this study can be effective for material deterioration.

## References

[1] Japan road association: Design specifications for steel highway bridges/Production specifications for steel high-way bridge, Gihoudo Co. Ltd., 1956.

[2] Japan road association: Specifications for highway bridges part2 steel bridges ver. 2002, Maruzen Co. Ltd., 2002.

[3] Masuya, H., Yokoyama, H., Sekiguchi, M., and Xu, C.: Study on impact behavior of fatigue deteriorated reinforced concrete slab by finite element method" Proceedings of 11th International Conference on Shock & Impact Loads on Structures, 267-272

[4] Nguyen T., N., Masuya, H., Xu, C., Kaii, H., Yamaguchi, T. and Yokoyama, H.: Self-propelled impact vibration equipment for the utilization of inspection of bridge deck, Proceedings of 9th symposium on decks of highway bridge, pp.89-92, Nov. 2016

[5] Shakushiro,K., Mitamura, H., Watanabe, T. and Kishi, N. : Experimental study on fatigue durability of RC slabs reinforced with round steel bars, Journal of structural engineering, JSCE, Vol57A, No.5, pp.1294-1304, March.2011

# Chapter 6: Conclusion

Currently, Falling Weight Deflectometer is one of the most popular method of Nondestructive testing method to evaluate the deterioration of structure. After a high speed grew up of the economy and scientific of technology, many civil structures were built. And theirs aging now is a challenge of not only developed country like Japan but also for developing country like Vietnam to evaluate and maintain. By Self-propelled impact vibration equipment (SIVE), a series of experiment has been done for estimate the degradation of structure which is highway concrete slab. After developing the equipment, it is assured that the abilities of SIVE in mobility in the field test, it is easy to examine any determine point. Moreover, its own power supply makes the test can do in any condition.

SIVE capability of changing the falling weight, falling height and rubber buffer makes SIVE can be suitable for many types of concrete slabs or structures. Chapter 2 shows the overall view of SIVE and the developed progress. The next chapter shows the experiment in two real bridges which are observed some degradation phenomenon. In chapter 4, using FEM to analysis the bridge to make sure the results of experiment and judges the accuracy of SIVE. The results of SIVE and analysis achieved in this study are summarized follow

(1) In the impact test, no difference in the feature of the displacement distribution in the bridge axis due to the load action time was observed. From the displacement distribution in the direction of the girder, it was found that the displacement of the loading point shows an abnormally large value, and it was suggested that the cause is due to the influence of the pavement. As a result of applying Newton’s interpolation for the loading point displacement measured from the pavement, rough agreement was found with the actual displacement measured from a high-precision displacement meter from the lower surface of the deck slab.

(2) Since it was suggested that the pavement displacement during the test did not show much change due to temperature and the displacement of the pavement

other than the loading point was almost the same as the displacement of the bridge slab. From the viewpoint of the pavement upper surface and the lower surface of the deck, as a result, it was shown that the deterioration situation of the deck can be estimated from the comparison of the experimental value of the displacement on the pavement upper surface and the analysis value in this study.

(3) When the damage progression is confirmed during the next bridge inspection, it is considered that an implementation of a similar load test at this time will be effective from the viewpoint of determining the degree of damage.

Subsequently, the degree of deterioration of slabs has been found out, a plan of maintenance is required. It is necessary to give a reasonable judgment method to select two ways, which specifically is the way ensuring the required performance by repair and reinforcement and the way to prolonging the life until the next countermeasure. Therefore, in this research, in order to provide the reinforcement method to improve load bearing performance and the method that can be expected to prolong life even if improvement of load bearing performance cannot be anticipated, experimental research had been done. By using Carbon Fiber Reinforced Polymer (CFRP) on the lower surface of the slab and confirming the reinforcing effect by the wheel load running experiment. The obtained results are shown

(1) Reinforced by CFRP is an effective method. The life of specimen was postponed by carbon fiber reinforcement in only the direction of the bridge axis. Reinforcing effect of 10.14 times as an equivalent to the number of running times was obtained. It is undenied that reinforcing by CFRP is sufficient not only in reinforcement but in economy problems as well.

(2) It has become clear that the reinforcing effect can be obtained only by reinforcement in the range where the load acts, because the strain of the carbon fiber of the specimen is large just under the wheel load and strain in the vicinity of the support is quarter.

(3) In the specimen with a small Young's modulus, the effect of reducing deflection by carbon fiber reinforcement in two directions was confirmed and it

is considered that an improvement in fatigue durability could be expected. However, in the confirmation of the quantitative effect, further examination is required.

In the future, we are going to conduct a confirmation experiments on fatigue durability by wheel load running experiment for deteriorated bridge slab by ASR, and we are planning to examine whether carbon fiber reinforcement shown in this study can be effective for material deterioration.